(NASA-CR-120739) PROCESS DEVELOPMENT FOR PRODUCING FINE-GRAIN CASTING IN SPACE Final Report (Battelle Columbus Labs., Ohio.)
68 p HC $4.25 CSCL 22A G3/12

N75-21313
Unclas
19239

RESEARCH REPORT

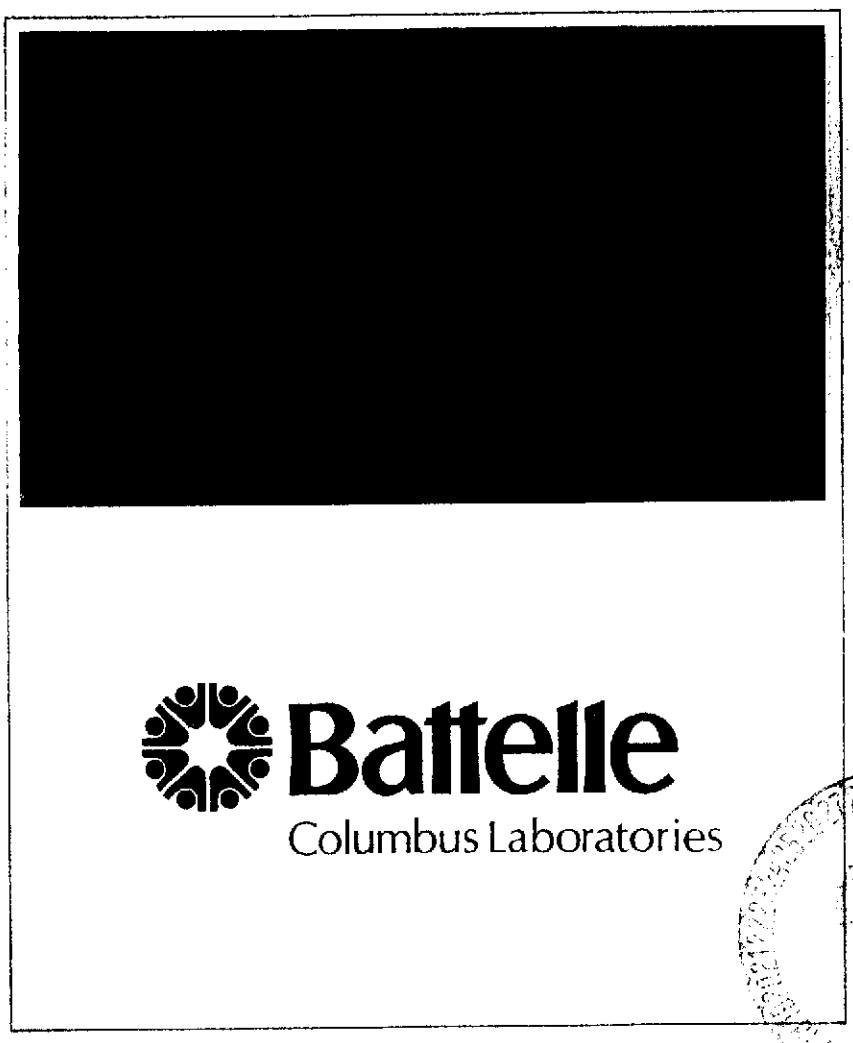

Battelle
Columbus Laboratories

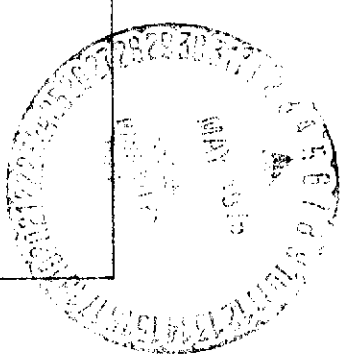

BATTELLE'S COLUMBUS LABORATORIES comprises the original research center of an international organization devoted to research and development.

Battelle is frequently described as a "bridge" between science and industry – a role it has performed in more than 90 countries. It conducts research encompassing virtually all facets of science and its application. It also undertakes programs in fundamental research and education.

Battelle-Columbus – with its staff of 2500 – serves industry and government through contract research. It pursues:

- research embracing the physical and life sciences, engineering, and selected social sciences
- design and development of materials, products, processes, and systems
- information analysis, socioeconomic and technical economic studies, and management planning research.

505 KING AVENUE • COLUMBUS, OHIO 43201

FINAL REPORT

on

PROCESS DEVELOPMENT FOR PRODUCING FINE-GRAIN CASTINGS IN SPACE

to

NATIONAL AERONAUTICS AND SPACE ADMINISTRATION
MARSHALL SPACE FLIGHT CENTER

April 10, 1975

by

S. H. Gelles and R. K. Malik

Contract No. NAS8-29626

BATTELLE
Columbus Laboratories
505 King Avenue
Columbus, Ohio 43201

ABSTRACT

An experimental study, the ultimate objective of which is to take advantage of the 0-g environment afforded by an orbiting spacecraft to produce a fine-grain beryllium ingot, is described. The approach originally envisioned was to distribute fine particles of BeO uniformly in molten beryllium by melting at low g a compact of beryllium powder containing BeO either naturally occurring on the particle surfaces or as a blended addition. It was anticipated that the 0-g environment would maintain the uniformity of the distribution of the oxide particles which would act as heterogeneous nucleating agents during solidification and so provide for a fine-grain beryllium ingot.

Initial melting experiments were conducted in the aluminum-aluminum oxide system as a mock-up for the beryllium-beryllium oxide system. Melting and solidification of aluminum-aluminum oxide powder compacts under controlled conditions coupled with careful characterization of the resulting structures by optical and transmission electron microscopy and by scanning electron microscopy showed that in terrestrial experiments the Al_2O_3 oxide, even where it had become highly concentrated, did not produce a fine grain size. Accordingly, further work was concentrated on the beryllium-beryllium oxide system where similar experiments also showed that no grain refinement was achieved in this system. Further experiments in this system were aimed at determining the reasons for the coarse-grained structure. Two possibilities were explored: (1) a rapid grain-growth rate in the solid near the melting point of beryllium and (2) a lack of effective heterogeneous nucleation sites.

Assessment of grain-growth kinetics at temperatures near the melting point and investigation into the use of potential nucleating agents in combination with the naturally occurring BeO led to the definition of critical low-g experiments which would help to determine whether one or both of these possibilities are valid and whether space processing would be able to yield fine-grain ingot beryllium.

FOREWORD

This is the final report on the program, "Process Development for Producing Fine-Grain Castings in Space", Contract NAS8-29626. This report covers the contractual period June 29, 1973, through April 10, 1975. Mr. I. C. Yates is the COR on this program. Experimental data from this program are reported in Laboratory Record Book Numbers 30778 and 31217.

TABLE OF CONTENTS

TABLE OF CONTENTS
(Continued)

LIST OF TABLES

LIST OF TABLES
(Continued)

LIST OF FIGURES

LIST OF FIGURES
(Continued)

FINAL REPORT

on

PROCESS DEVELOPMENT FOR PRODUCING FINE-GRAIN CASTINGS IN SPACE

to

NATIONAL AERONAUTICS AND SPACE ADMINISTRATION
MARSHALL SPACE FLIGHT CENTER

from

BATTELLE
Columbus Laboratories

by

S. H. Gelles and R. K. Malik

April 10, 1975

INTRODUCTION

The overall objective of this program is to take advantage of the low-g environment afforded by space to produce a fine-grain beryllium cast product--a feat which has been elusive in the terrestrial environment but could lead to the production of beryllium hardware items of near-net shape and good mechanical behavior.

When the program was initiated, it was believed that the obstacle to achieving a fine-grain cast beryllium product was a lack of nucleation sites. Accordingly, the original plan was to produce a melt containing a dispersion of beryllium oxide which would be suspended uniformly in the liquid bath due to the lack of gravitational settling forces and gravity-driven convection currents. The oxide was intended to act as a heterogeneous nucleating agent as well as a grain-growth inhibitor in the solid during cooling. The possibility was also considered that the dispersed oxide would contribute to the strength of the metal, especially at elevated temperature.

It was originally intended that during the present program, effort would be concentrated on the aluminum-aluminum oxide system as a mock-up

for the beryllium-beryllium oxide system. These systems are similar with respect to the high stability of the oxide and the low solubility of oxygen in the molten metal. However, the experiments conducted with the aluminum-aluminum oxide system showed that grain refinement by dispersing oxide in molten aluminum was not achieved, even in regions of the samples containing high concentrations of alumina.

When this was discovered, the program emphasis was shifted to the beryllium-beryllium oxide system with the oxide introduced either as the BeO occurring naturally on the surfaces of beryllium powder particles or as an addition of fine BeO powder. Here again, the presence of various concentrations of oxide did not produce a fine-grain ingot material, the behavior being attributed to either the lack of nucleating sites and/or the rapid grain growth occurring in solid beryllium at temperatures just below the melting point. A program was delineated to establish whether either or both factors were important.

A study of the kinetics of grain growth in beryllium powder compacts and fully dense powder metallurgy samples produced from Kawecki Berylco Industries P-1 beryllium powder showed that very little grain growth occurred up to the melting point. It was thus tentatively concluded that grain growth in the solid just below the melting point was not the cause of the large grain size in the ingot beryllium. Accordingly, a series of experiments was conducted in which various potential nucleating agents, mainly compounds which had at least a fair lattice parameter match with the allotrope of beryllium existing just below the melting point, were investigated.

None of the inoculants produced significant grain refinement in the melted and solidified powder billets. This was interpreted as being due to one or both of the following conditions:

(1) The inoculants are ineffective as nucleating agents.

(2) The grain-growth inhibiting action of the BeO is detroyed during the melting process.

The second condition is rather plausible in the light of recently published results[1] linking grain growth in powder metallurgy beryllium with the agglomeration of the oxide particles present in the structure. This cited research provided us with the incentive to examine the BeO present in the powder compacts before and after melting. The transmission electron microscope study revealed that in both the melted and unmelted cases, a beryllium oxide network existed in the metal. However, the oxide in the melted material was appreciably coarser than in the unmelted material. This is believed to be the reason for unrestricted grain growth in the ingot metal.

The agglomeration of the beryllium oxide appears to require the present of a liquid phase. In some grades of beryllium in which the concentrations of the low melting elements, silicon, aluminum, or magnesium, are not kept sufficiently low, incipient grain-boundary melting occurs and is accompanied by agglomeration of the BeO inclusions present in the powder metallurgy products. In such products, grain growth occurs well below the melting point of beryllium. The particular beryllium powder used in this investigation was probably of sufficiently high purity to minimize any incipient melting and oxide agglomeration, even at temperatures very close to the beryllium melting point. However, once general melting occurred, oxide agglomeration resulted; and the oxide no longer acted as a grain-growth inhibitor.

There is good reason to believe that oxide agglomeration occurs as a result of collisions of the small oxide particles in a liquid medium. The liquid can be distributed either in a localized region, as might occur in incipient melting, or might be present on a larger scale, as would be the case when general melting occurred. Agglomeration of the oxide by collision processes should be almost exclusively gravity driven although velocity gradients and resulting collisions may conceivably occur during solidification. Collisions are produced when particles move in the fluid at different velocities. Two major collision mechanisms are probable.

(1) Stokes Flow. The settling or rising of particles in a fluid due to density differences between the

particle and the fluid. The flow velocity is proportional to the square of the particle diameter. Collisions occur between particles of different diameters.

(2) Velocity Gradients. These result from gravity-driven convection currents caused by density gradients in the fluid.

This type of behavior is currently being analyzed on another NASA program dealing with immiscible materials.[2]

The fact that oxide agglomeration should occur primarily as a result of gravity-driven collision processes provides an opportunity to test in critical low-g experiments some of the hypotheses we have set forth dealing with nucleation and grain-growth problems in beryllium. Thus, we have described in this report two basic experiments to be conducted in a drop tower or sounding rocket which should isolate the problems associated with attaining a fine-grained ingot beryllium.

In the first, a beryllium powder compact containing the natural occurring surface oxide would be melted and rapidly solidified in a manner similar to that carried out at 1 g. Samples would be examined metallographically for evidence of a fine-grain ingot structure. If the results are positive and if the oxide is found not to be appreciably changed, we would conclude that

(1) The oxide provided a sufficient number of nucleation sites during solidification for producing a fine-grain metal.

(2) The low-g environment prevented agglomeration of the oxide so that grain-growth inhibition was maintained.

If, on the other hand, no grain refinement was observed but the oxide remained unagglomerated, it could be concluded that too limited a number of effective nuclei were present and that the inoculant experiments should be repeated at 0 g and if necessary extended to other materials.

Lastly, if neither grain refinement nor prevention of oxide agglomeration is observed, it would be necessary to reevaluate the entire theoretical framework dealing with grain nucleation, crystal growth, and grain-growth inhibition in this system.

BACKGROUND

As-cast beryllium usually has a grain structure which is both large and columnar. This material is weak and brittle in the as-cast condition. It is only by heavy working that the grain structure can be refined and usable properties achieved. Ingot beryllium is usually induction melted and cast and during the process the beryllium oxide, which was present on the surfaces of the melting stock, is usually removed from the interior of the molten bath to the surface of the melt and held there by surface tension. Thus, the bulk of a vacuum-melted beryllium ingot contains very low oxygen levels, and since BeO is a known grain-growth inhibitor in beryllium, its absence allows excessive grain growth to occur during cooling from the solidification temperature.

Another reason for the large grain size present in ingot beryllium may be the lack of effective heterogeneous nucleating agents that may provide a multiplicity of sites at which individual grains can nucleate. A small number of programs have been carried out in the past which have explored the use of heterogeneous nucleation agents to produce fine-grain ingot beryllium.[3-5] In some cases, these elements and compounds were selected on the basis of empirical scientific principles governing selection of effective nucleating agents.[6,7] Two basic principles were considered.

(1) The mismatch between the lattice parameters of the nucleating agent and that of the solid being nucleated should not be large.

(2) The interfacial energy between the crystallizing solid and the nucleating agent should be much smaller than the interfacial energy between the liquid and the nucleating agent.

A small number of studies have been conducted in this area with relatively little success.[3-5] Although there have been claims made that inoculants such as tantalum nitride, boron nitride, titanium diboride, tungsten carbide, and beryllium oxide refine the grain structure either alone or in combination with soluble elements such as aluminum or silicon, the grain size in the treated billets is not sufficiently refined to be of interest (200 to 400 μ).

The mechanical behavior of beryllium is a very sensitive function of the grain diameter, d. In general, both yield and ultimate tensile strengths increase linearly with $1/d^{1/2}$, the usual Hall-Petch relation.[8] The dependence of ductility on grain size is more complicated since it is related to the ductile-brittle transition temperature. This, in turn, decreases with decreasing grain size although not in a linear fashion.[9] Accompanying the decrease in ductile-brittle transition temperature is a general increase in ductility in the temperature range below the transition. For beryllium having a random grain orientation, a 10-μ grain size (achievable in powder metallurgy compacts) will produce ductilities in all directions of about 2 to 5 percent. It is estimated that increasing the grain size much above 50 μ will produce a metal having extremely low ductilities (few tenths of a percent). Thus, the grain sizes achieved thus far in the past inoculation studies[3-5] are not sufficiently fine to produce a material with attractive mechanical properties. Further refinement of the grain size is required for the utilization of beryllium castings.

If the technology of producing fine-grain beryllium castings is successfully developed, we would anticipate the achievement of economical benefits over the powder metallurgy route currently being used exclusively in the production of intricate beryllium components.

The cost of raw beryllium is presently ∿ \$60-\$140 per lb (\$132-\$308 per kg). In fabricated form the price can easily exceed \$1000 per lb (\$2200 per kg). It is likely that the savings gained through successful development of the beryllium casting technology based on space processing will more than cover the added space transportation costs, at the very least for the complex parts.

EXPERIMENTAL PROGRAM

Aluminum-Aluminum Oxide Studies

Outline of Studies

The aluminum-aluminum oxide system was explored as a low melting point model for the beryllium-beryllium oxide system to verify the concept that a distribution of oxide in a solidifying metal might provide the nucleation sites and the grain-growth inhibition which would lead to a fine-grain ingot material.

The material variables studied were oxide content, size, and distribution. The aluminum oxide was introduced in two forms:

(1) As the naturally occurring, very fine oxide present on the surface of aluminum-powder particles

(2) As an addition of aluminum oxide powder.

The concentration of oxide was controlled by the oxide content of the aluminum powder used and by the amount of the addition. The distribution of oxide in the structure was varied by utilization of different sizes of aluminum powder. Accordingly, the following four materials were evaluated:

(1) -100+325 mesh aluminum powder containing $\sim$ 1% of naturally occurring aluminum oxide

(2) The same powder into which was blended $\sim$ 2 vol % of -100+325 mesh aluminum oxide powder

(3) -325 mesh aluminum powder containing 1% aluminum oxide

(4) The same powder as (3) into which was blended $\sim$ 2 vol % -325 mesh aluminum oxide powder.

Two other variables concerned with the melting operation were also investigated. These were the maximum melt temperature and the cooling rate. The first of these was to provide a baseline measurement for the heat transfer characteristics associated with the melting operation. The

variation of the cooling rate was aimed at determining what effect this parameter had on the ultimate grain structure. The melting and solidification parameters were to be well documented by means of thermal analysis, and the structural changes were to be determined by examination of the melted and solidified materials and by study of the resultant distribution of the oxide and the effect of the oxide on the grain structure.

Materials

Two lots of high-purity aluminum powder were provided by ALCOA. One lot (Grade 7101) was intended to be -100 mesh, and a second lot (Grade 7123) was expected to be essentially -325 mesh. Typical characteristics of these powder grades are provided in Tables 1 (particle size distribution) and 2 (chemical analysis).

From inspection of Table 1, it is seen that most of Grade 7101 was of the -325 mesh size fraction. However, enough of the powder was in the -100+325 mesh size range to provide the coarser material for this study.

From Table 2 it may be seen that the typical content of impurities other than Al_2O_3 is quite low. The combined level of Al plus Al_2O_3 is close to 99.99 percent.

Oxygen analyses have been obtained from Intelcom Rad Tech for the two as-received lots as well as the coarse fraction of the Grade 7101 powder. These analyses are shown in Table 3 and indicate that the oxide content is in the intended range.

The two major materials studied in this program were the -100+325 and -325 mesh fractions of Grade 7101 powder chosen because of the higher oxide content. However, some preliminary experimentation was conducted on the -325 mesh Grade 7123 powder.

Scanning electron microscope (SEM) studies have been conducted on as-received and sized powders in order to characterize the size distribution, particle morphology, and if possible the oxide size and morphology. As may be seen in Figure 1, the powder particles are irregular but generally rounded in nature. The difference in size distribution

TABLE 1. TYPICAL PARTICLE SIZE ANALYSIS OF AS-RECEIVED ALCOA ALUMINUM POWDERS[a,b]

Grade	Screen Analysis, percent			Average Particle Diameter Fisher Subsieve Sizer	Mass Median Diameter Sharples Micromerograph	Surface Area, m^2/g
	-100+200 Mesh	-200+325 Mesh	-325 Mesh			
7101	0 - 5	10 - 25	75 - 90	17 - 24	34	.15 - .25
7123	0	1 - 10	90 - 99+	15 - 19	29	.20 - .30

(a) ALCOA Form 30-12817, Rev. 7/71.

(b) ALCOA Product Sheet, "ALCOA High-Purity Atomized Powders, Grades 7120; 7101; and 7123".

TABLE 2. TYPICAL CHEMICAL ANALYSIS OF AS-RECEIVED ALCOA ALUMINUM POWDERS, PERCENT BY WEIGHT[a]

Element	Grade 7101	Grade 7123
Al	99.391	99.391
Al_2O_3	0.6	0.65
Fe	0.002	0.002
Si	0.002	0.002
Others, total	0.005	0.005

(a) ALCOA Product Sheet, "ALCOA High-Purity Atomized Powders, Grades 7120; 7101; and 7123".

TABLE 3. NEUTRON ACTIVATION ANALYSIS OF OXIDE CONTENT OF ALUMINUM POWDER[a]

Material	Oxide Content, wt %
Grade 7101 As-Received (-100 mesh)	0.948
Grade 7101 -100+325 fraction	0.943
Grade 7123 As-Received (-325 mesh)	0.667

(a) Analysis performed at Intelcom Rad Tech, San Diego, California.

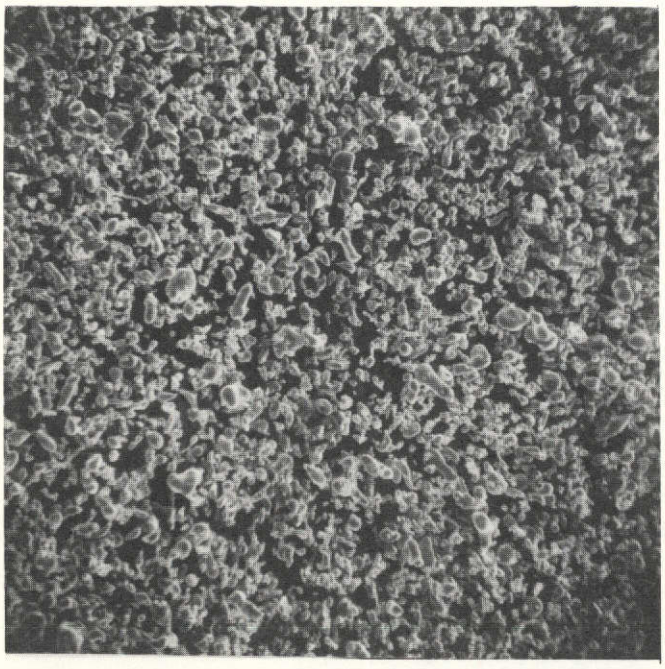

100X 307

a. -325 Mesh

100X 310

b. -100 +325 Mesh

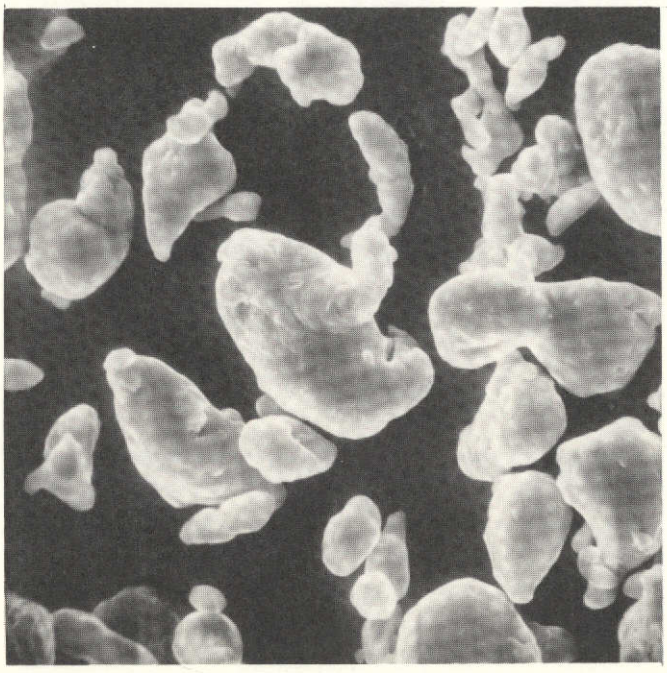

1000X 309

c. -325 Mesh

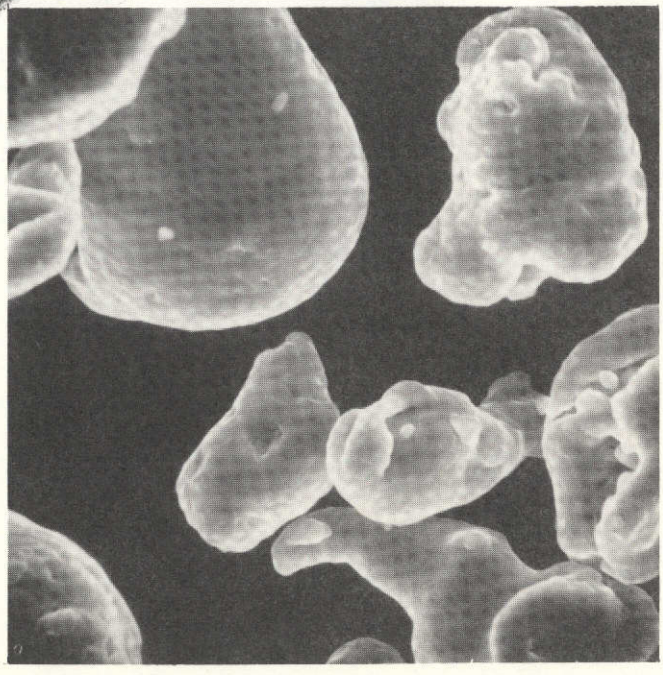

1000X 312

d. -100 +325 Mesh

FIGURE 1. SEM PHOTOGRAPHS OF TWO SIZE FRACTIONS OF GRADE 7101 ALUMINUM POWDER

between the -100+325 and the -325 mesh powder is also obvious by comparison of Figures 1a and 1c with 1b and 1d, respectively. The oxide distribution in the powders is not obvious from the SEM examination of the powder surfaces. However, it is conceivable that the smaller particles on the surface of the large particle in Figure 1d are some of the coarser oxide particles.

High-purity Al_2O_3 powder was provided to the program in two size ranges (-100+325 mesh and < 1-μ median particle size) by ALCOA, East St. Louis, Illinois. Typical chemical analyses of the unground and superground XA-139 Al_2O_3 powder are listed in Table 4.

In addition, the superground XA-139 Al_2O_3 powder was examined in the electron microscope. The particles examined were angular and ranged in size between 0.02-0.4 μ. The selected area diffraction pattern agreed with that of the trigonal α-Al_2O_3 in confirmation of the ALCOA literature.

Thermal Analysis Method

Melting and solidification experiments were conducted with the equipment illustrated in Figure 2. It consisted of a furnace and controller, Vycor tube, vacuum system, thermocouples, and a millivolt recorder. The sample, a compact of aluminum powder produced by isostatic pressing at 689 MPa (100 ksi), was approximately 1.3 cm in diameter x 1.3 cm long. It contained a blind axial hole 5 mm in diameter that extended half its length and was designed to fit snuggly into a tantalum crucible containing a 3.18-mm (1.8-in.) thick end plate. The end plate contained a closed-end tantalum tube 4.73 mm in diameter (0.186 in.) which mated with the blind hole in the compact. This latter arrangement was used as a recess hole for a thermocouple which was used to monitor the temperature-time history of the sample and which acted as a support for the crucible and sample. The entire sample-thermocouple assembly was contained in a Vycor tube 57-mm OD rigidly fastened to a supporting frame. The tube was attached to a vacuum system which was capable of achieving vacua of better than 10^{-5} Torr. A resistance wound furnace 40 cm long with a 6.3-cm-diameter opening was suspended vertically and counterbalanced over a set of pulleys.

TABLE 4. CHARACTERISTICS OF XA-139 Al_2O_3 POWDER

ALCOA Provided Data

Compound	Analysis, wt % Unground	 Superground
SiO_2	.012	.026
Fe_2O_3	.008	.009
TiO_2	<.001	<.001
Na_2O	.006	.005
CaO	.006	.008
Ga_2O_3	.003	.003
B_2O_3	<.001	<.001
MnO	.0006	.0005
Cr_2O_3	.0002	.0002
MgO	.0005	.0106
ZnO	<.0005	<.0005
CuO	<.0005	<.0005
V_2O_3	<.0001	<.0001
Al_2O_3 (diff.)	<99.956	<99.932
Size	-100+325 mesh	Median < 1 μ

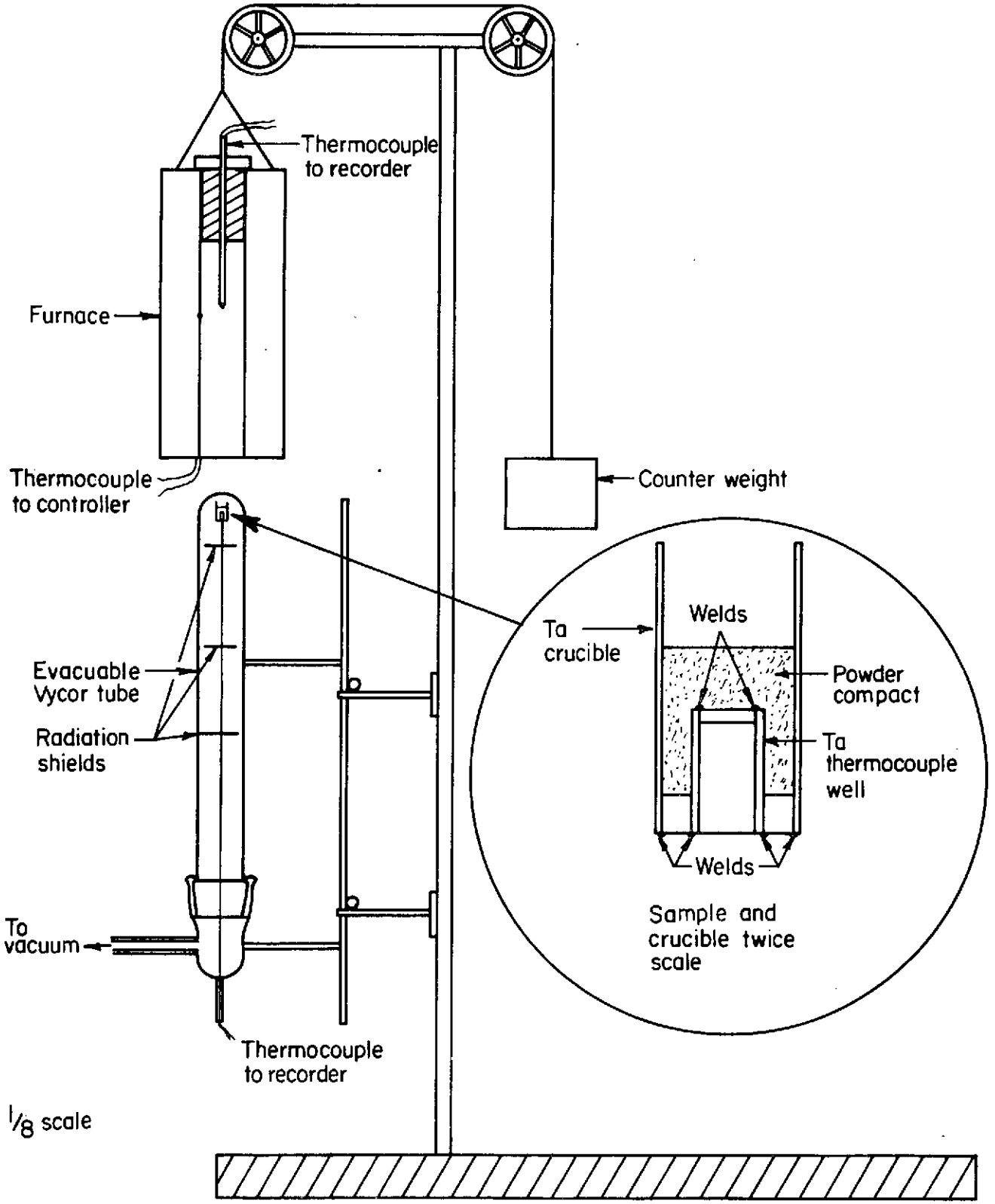

FIGURE 2. SCHEMATIC DRAWING OF THERMAL ANALYSIS EQUIPMENT AND SAMPLE

The furnace was thus easily positioned in relationship to the sample. This arrangement allowed the furnace to be preheated in a position displaced vertically from the sample and then to be lowered in order to melt the sample. Rapid cooling of the sample at the conclusion of an experiment was effected by raising the furnace from the sample, whereas slow cooling was accomplished by leaving the furnace in place and shutting off the power.

In a typical melting and solidification experiment, the machined compact was placed in a tantalum crucible provided with a thermocouple well (see insert, Figure 2) and the crucible placed on the thermocouple support within the fused silica tube which was subsequently evacuated to $\sim 1 \times 10^{-5}$ Torr. The furnace was then heated to a convenient temperature above the melting point of aluminum (usually 750 C) while being suspended just above the fused silica tube. After the furnace had been equilibrated at temperature, it was then lowered around the tube and sample and the temperature recorded as a function of time. Melting of the sample was detected by an easily distinguished plateau in the temperature-time record. Heating was continued until the sample reached the equilibrated furnace temperature. At this point the sample was cooled by either shutting off the furnace (slow cool) or by raising the furnace so that the sample was no longer in the hot zone (fast cool). The samples were then cooled through the solidification plateau to room temperature or in some instances were recycled additional times through the melting and solidification range.

Preliminary Experiments

Thermal Analysis. An initial set of experiments was conducted on three compacts made from -325 mesh aluminum powder (Grade 7132) in order to check the operation of the equipment and the experimental procedures. These experiments were conducted with a furnace preheated to 750 C.

Table 5 summarizes the preliminary melting and solidification experiments and includes the heating rates just prior to melting, the

TABLE 5. SUMMARY OF PRELIMINARY MELTING AND SOLIDIFICATION EXPERIMENTS(a)

Specimen No.	Cycle No.	Heating Rate, deg C per sec	Melting Temperature Range, deg C	Cooling Rate, deg C per sec	Solidification Temperature Range, deg C
TA-1	1	0.86	642-675	1.14	619-586
TA-2	1	0.71	673-653-678	1.97	633-590
TA-3	1	2.36	681-689	2.05	648-610
TA-3	2	1.49	662-681	0.64	624-609
TA-3	3	0.94	654-676	0.094	656-646
TA-3	4	0.39	655-667	0.11	655-647

(a) Compacts of -325 mesh aluminum powder (Grade 7132).

cooling rates just before solidification, and the measured melting and solidification ranges. It is obvious from these data that the apparent melting and solidification temperatures vary significantly from the equilibrium, the deviations increasing with increasing heating and cooling rates. There is no evidence from the cooling curves that this effect is related to supercooling. It is apparently caused by the larger temperature gradients associated with the faster rates, the somewhat imperfect contact between the thermocouple bead and sample, and a larger thermal inertia of the sample compared to the thermocouple.

Structural Analysis. Metallographic inspection of Samples TA-1 and TA-2 revealed similar structures consisting of coarse-grain regions essentially devoid of a second phase and regions near the tantalum crucible walls which had relatively high concentrations of a second phase (presumably Al_2O_3) and which appeared to be a fine-grain structure. These latter regions are shown as the white band in the dark-field micrograph of Figure 3c. This result was quite encouraging since it appeared to support our hypothesis that the presence of the oxide would produce a fine-grain structure. In a later part of our study, however, we discovered that the regions interpreted as being fine grain were, in fact, rather coarse grain areas consisting of fine dendrites.

Final Experiments

Thermal Analysis. The main body of thermal analysis experiments conducted on the aluminum-aluminum oxide powder compacts is summarized in Table 6. The experiments summarized represent a combination of material variables (Materials 1, 2, 3, and 4), two different cooling rates (fast cool, F; and slow cool, S), and two maximum melt temperatures (750 (T_1) and 850 C (T_2)). The last parameter leads to a small variation in both heating and cooling rates (see Table 7).

As may be seen from Tables 6 and 7, the major effect found from the thermal analysis work was similar to that found in the preliminary thermal analysis experiments; namely, the apparent melting and solidification temperatures were dependent in a highly reproducible way on the heating and cooling rates.

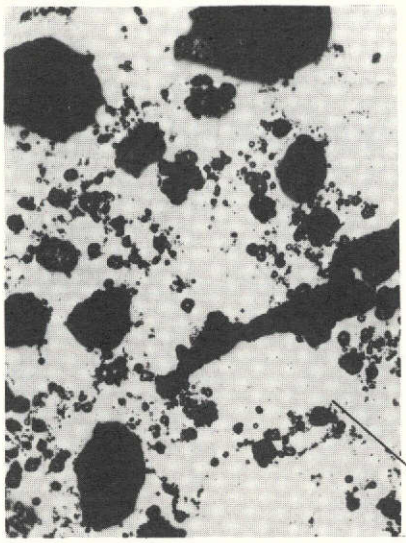

175X a. 8G373

175X b. 8G372

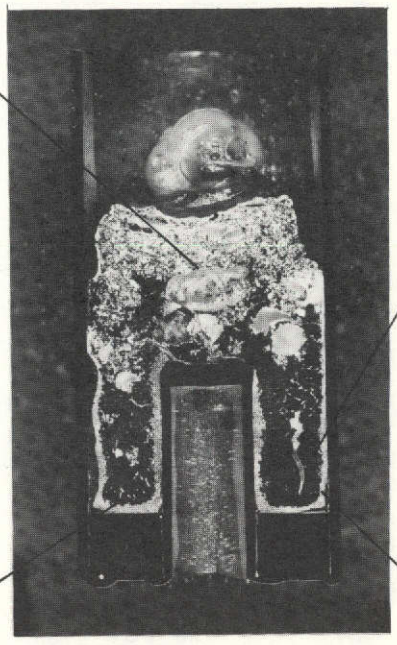

2.75X c. 8G377

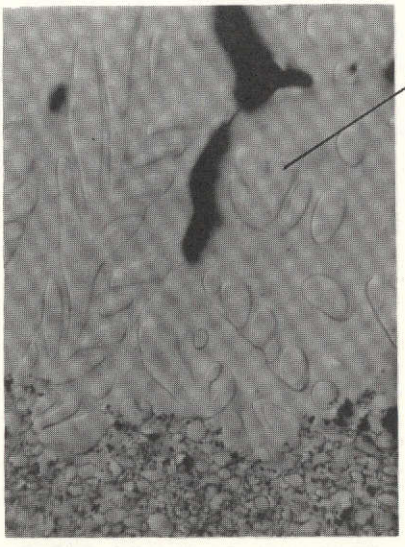

70X d. 313

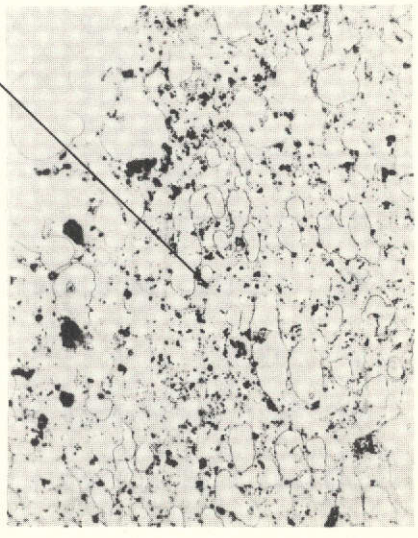

175X e. 8G371

FIGURE 3. PHOTOMICROGRPAHS OF SAMPLE TA-1

A, b, d, and e bright light; c dark field. Note fine-grain regions having a high concentration of second phase and coarse-grain regions free of second phase.

TABLE 6. SUMMARY OF THERMAL ANALYSIS EXPERIMENTS CONDUCTED ON ALUMINUM POWDER COMPACTS

Material[a]	Experimental Condition[b]	Run No.	Melting Range, C	Solidification Range, C	Heating Rate, C/sec	Cooling Rate, C/sec
1	T_1F	19	666-678	645-623	1.37	1.81
	T_1S	15	675-684	655-647	1.04	0.10
	T_2F	13	688-690	(c)	1.54	(c)
	T_2S	14	682-693	655-649	1.75	0.09
2	T_1F	6	670-681	650-612	1.29	1.75
	T_1S	16	668-678	654-646	1.35	0.09
	T_2F	12	684-699	645-614	1.84	2.52
	T_2S	17	678-692	657-652	1.94	0.09
3	T_1F	9	675-679	646-614	1.19	1.80
	T_1S	18	(c)	659-652	(c)	0.09
	T_1S	20	668-671	659-642	1.15	0.10
	T_2F	10	683-693	643-614	1.86	2.42
	T_2S	11	670-680	656-648	1.48	0.09
4	T_1F	4	667-673	649-613	1.13	1.86
	T_1S	5	672-678	655-646	1.02	0.10
	T_2F	7	678-687	646-622	1.94	2.30
	T_2S	8	688-693	659-650	1.91	0.09

(a) Material Code:

(1) -100+325 mesh aluminum powder (Grade 7101)

(2) Material (1) plus 2 vol % Al_2O_3 (XA-139 unground)

(3) -325 mesh aluminum powder (Grade 7101)

(4) Material (3) plus 2 vol % Al_2O_3 (XA-139 superground).

(b) Heating and Cooling Code: T_1 and T_2 are the maximum temperatures to which the melt is heated. T_1 = 750 C and T_2 = 850 C. F, S--fast or slow cool from this temperature, respectively.

(c) Poor recording.

TABLE 7. AVERAGE MELTING AND SOLIDIFICATION TEMPERATURE FOR VARIOUS HEATING AND COOLING CONDITIONS

Condition	Heating: Average Heating Rate, C/sec ± 1 σ	Midpoint of Recorded Melting Range, C ± 1 σ
Furnace preheated to 750 C	1.19 ± 0.13	674.4 ± 4.0
Furnace preheated to 850 C	1.78 ± 0.18	686.1 ± 5.3
Condition	**Cooling: Average Cooling Rate, C/sec ± 1 σ**	**Midpoint of Recorded Solidification Range, C ± 1 σ**
Furnace preheated to 750 C		
Fast cooling rate	1.81 ± 0.45	631.5 ± 1.7
Slow cooling rate	0.096 ± 0.005	651.6 ± 2.2
Furnace preheated to 850 C		
Fast cooling rate	2.41 ± 0.11	630.7 ± 2.9
Slow cooling rate	0.090 ± 0.000	653.3 ± 1.4

The furnace preheat temperature, either 750 or 850 C, made only a small difference in the heating and cooling rates. There was no measurable difference in thermal response among the four material variations investigated.

Structural Analysis. Examination of the macrostructure of the various Al-Al_2O_3 ingots processed in the thermal analysis experiments revealed only subtle differences arising from the variation in material parameters or resulting from variations in the processing. The most notable macroscopic effect was observed in Materials 3 and 4 in the distribution of the oxide. In those samples heated to the lower maximum temperature, there was a much larger concentration of oxide along the crucible side walls, thermocouple well, and crucible bottom than in comparable material processed at the higher maximum temperature. This effect appeared to be independent of the cooling rate. As expected, the concentration of oxide near the walls was higher in Material No. 4, which contained 2 vol % of additional Al_2O_3 than in Material No. 3. Figure 4 shows these effects on Materials 3 and 4 which have been slow cooled from approximately 850 C (T_2) or 750 C (T_1). As illustrated in Figure 5, photomicrographs of regions near the crucible base and thermocouple well confirm the general result for these materials that the oxide is less concentrated in the material processed at the higher maximum temperature.

The major microscopic difference observed was in the grain structure. Studies of Material 4 showed that the grain size was determined almost exclusively by the cooling rate. Figure 6 shows that at fast cooling rates ($\sim$ 2 C per sec) the grain size is significantly finer than in the samples cooled slowly ($\sim$ 0.1 C per sec). The maximum melt temperature appears to have little effect on the grain size over the temperature range studied.

The samples for grain size observation have been specially prepared by anodization in a 2.5 percent solution of fluoroboric acid at 20 v with an aluminum cathode and have been observed in polarized light. The optically anisotropic oxide, which assumes an orientation dependent on that of the underlying metal, allows the grain structure to be easily observed.

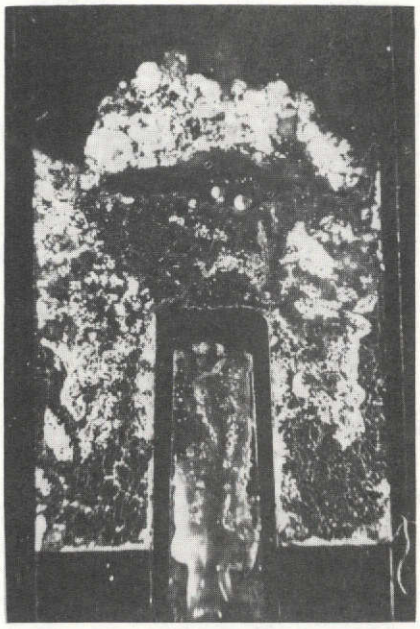

344

a. Material 3

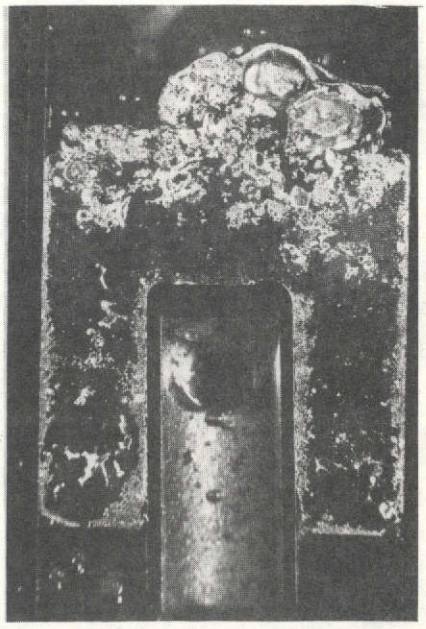

346

b. Material 4

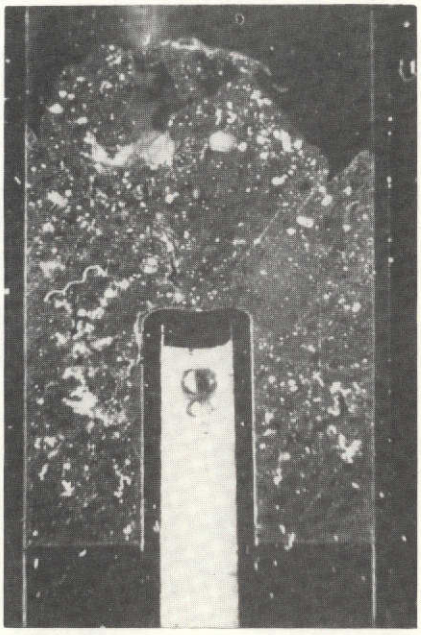

348

c. Material 3

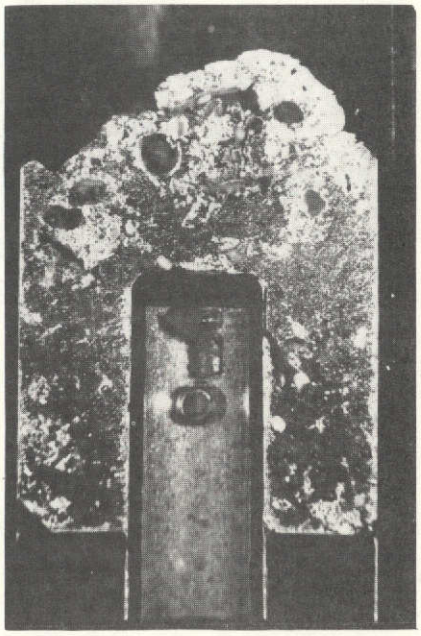

350

d. Material 4

FIGURE 4. MACROSTRUCTURES OF SECTIONED Al-Al_2O_3 INGOTS SLOW COOLED FROM MAXIMUM TEMPERATURES OF NOMINALLY 750 C (A, B) OR 850 C (C, D)

Etch - 20 Percent NaOH; 56X

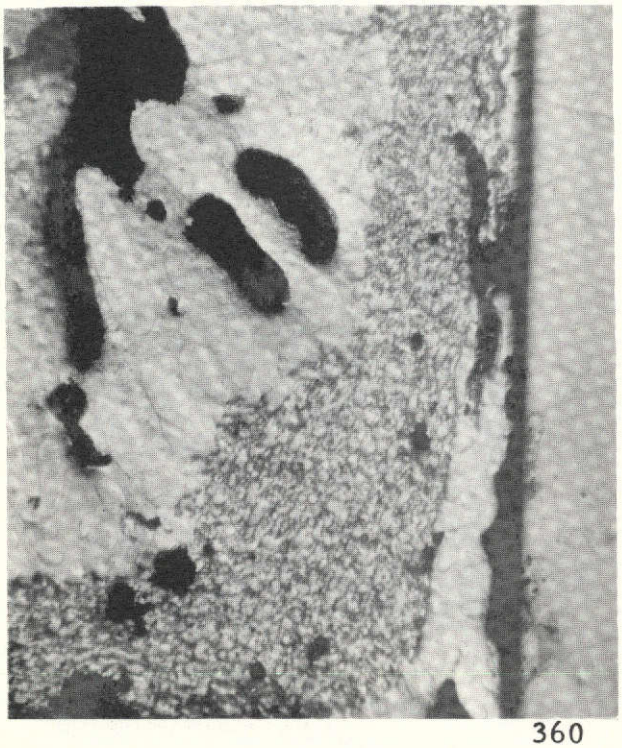

360

a. T_1F

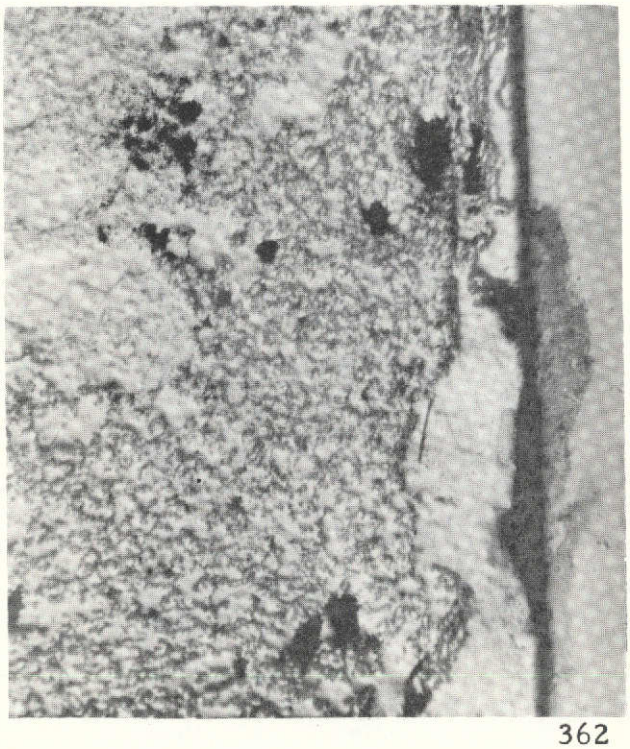

362

b. T_1S

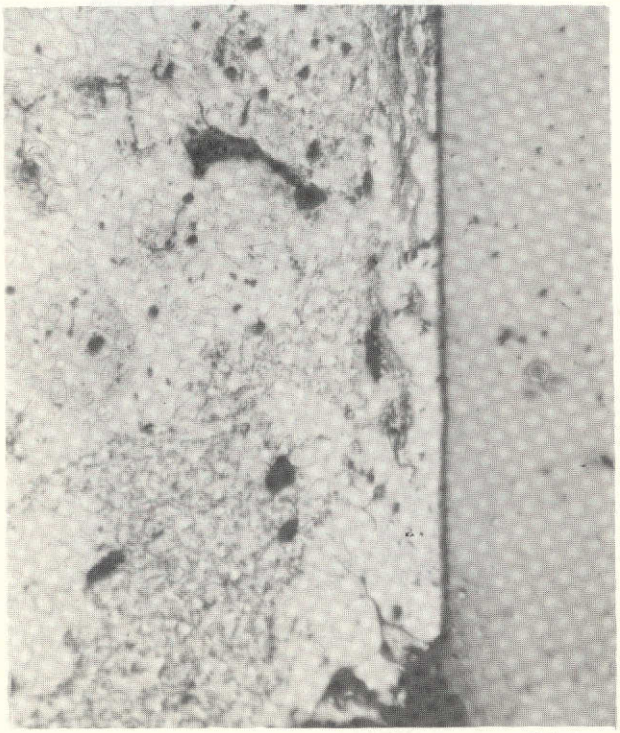

364

c. T_2F

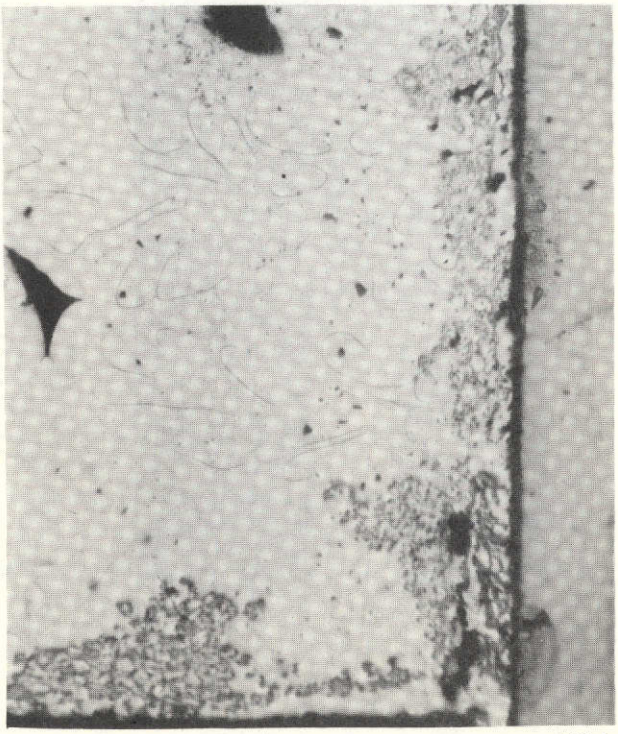

366

d. T_2S

FIGURE 5. MICROSTRUCTURES OF Al-Al_2O_3 MATERIAL 4 PROCESSED AT NOMINALLY 750 C (T_1) OR 850 C (T_2) AND GIVEN A FAST (F) OR SLOW (S) COOL THROUGH SOLIDIFICATION

Etch - 20 Percent NaOH; 56X

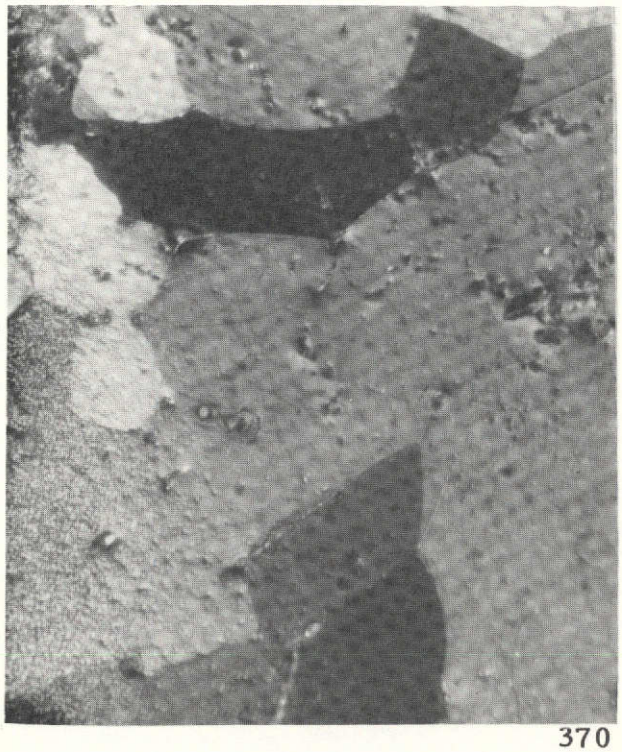

370

a. T_1F

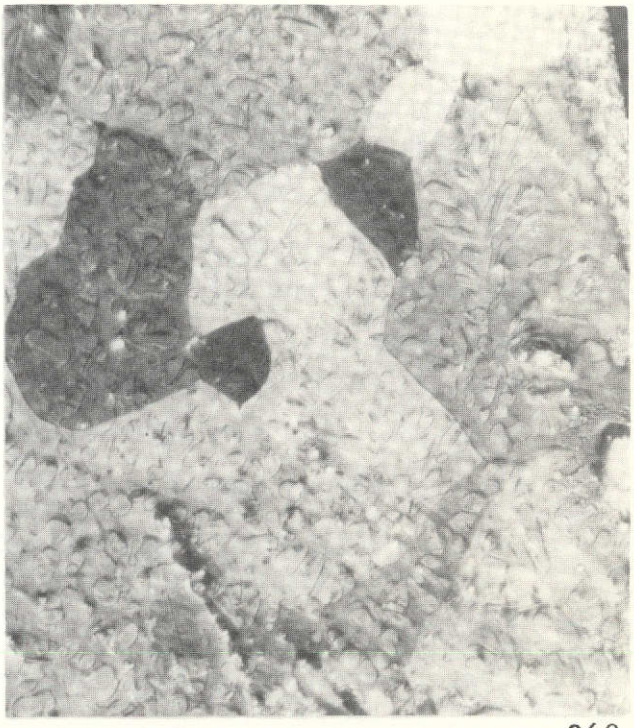

368

b. T_2F

371

c. T_1S

369

d. T_2S

FIGURE 6. MICROSTRUCTURES OF Al-Al_2O_3 MATERIAL 4 PROCESSED AT NOMINALLY 750 C (T_1) OR 850 C (T_2) AND GIVEN A FAST (F) OR SLOW (S) COOL THROUGH SOLIDIFICATION

Anodized, Polarized Light, 56X

Although the grain size of the rapidly cooled samples was somewhat finer than of those that had been slowly cooled, it is still very large. It is also large even in regions containing high concentrations of oxide. For example, the region marked with "A" in Figure 6d is all part of the dark large grain. Associated with the high concentration of oxide is a fine structure which had previously been attributed to a fine grain size. It is now clear that this is not the case and that the fine structure is due to a fine dendrite spacing in the high oxide region.

Characteristics of Al_2O_3 Present in Melted Al-Al_2O_3 Compacts.

Transmission and scanning electron microscopy were used to characterize the as-received Al_2O_3 and the morphology, distribution, and crystal structure of Al_2O_3 in some of the melted Al-Al_2O_3 powder compact.

Thin longitudinal sections of melted sample TA-2 were prepared in the following manner:

(1) Slice a 3-mm-thick sample from billet.

(2) Mechanically polish on abrasive paper to $\sim$ 1-mm thickness.

(3) Chemically mill in 20 percent aqueous solution of NaOH to $\sim$ 0.2 mm.

(4) Punch 3-mm discs from thinned section.

(5) Jet polish with Fischione Twin Jet Electropolishing Unit.

Some difficulty was encountered in polishing the samples, owing to the presence of porosity. However, we were able to successfully view some sufficiently thin regions in our Hitachi HUllE electron microscope at an accelerating voltage of 125 kv.

Transmission electron micrographs of the network of oxide particles are shown in Figure 7a, b, and c. Figure 7d is a region containing little oxide and shows the dislocation cell structure present in the material. Some of the oxide network extended into the hole perforated during the electrolytic thinning process and allowed a more detailed examination of the oxide, including selected area electron diffraction (SAD). Figure 8a is an electron micrograph of such a region; the

a. 2939

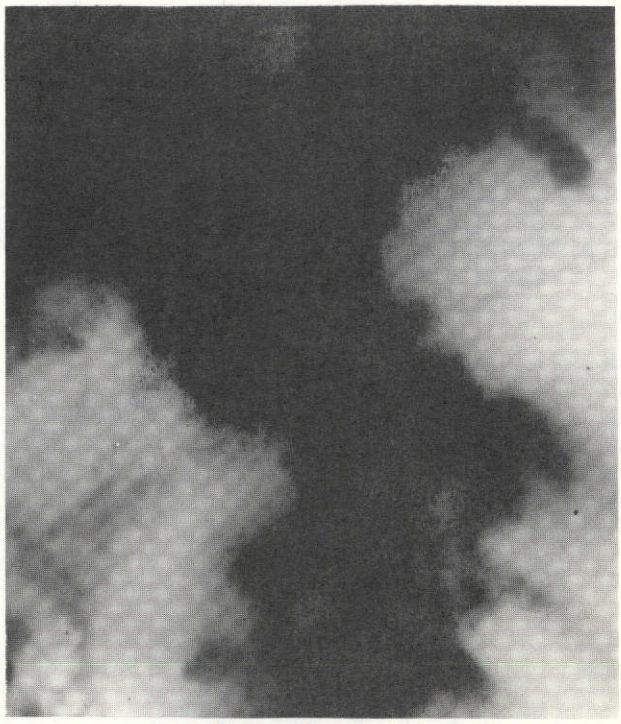

b. 2943

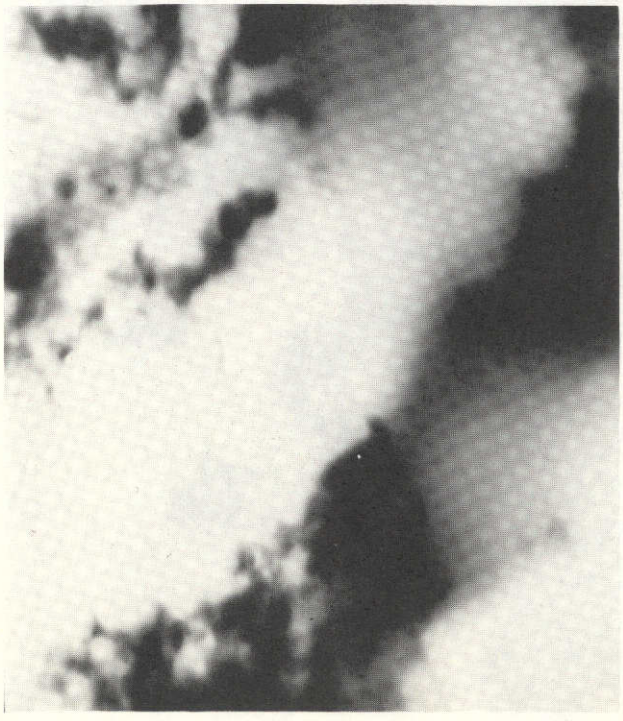

c. 2941

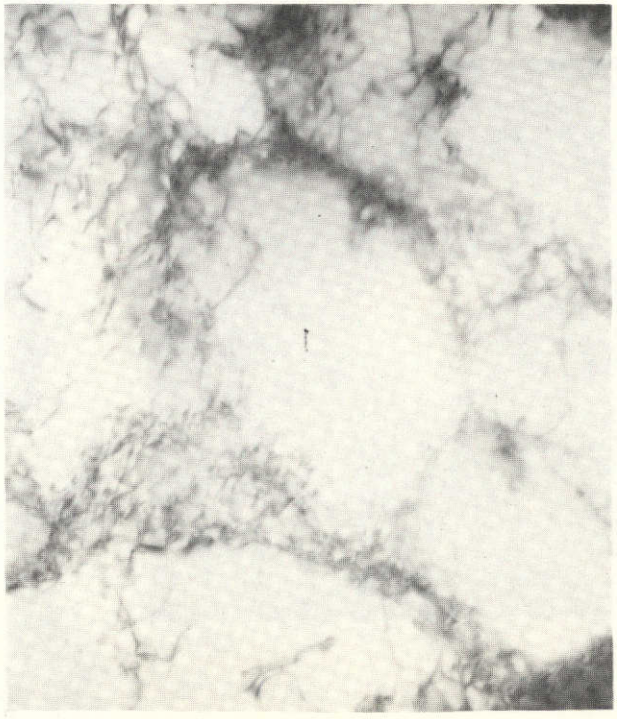

d. 2924

FIGURE 7. TRANSMISSION ELECTRON MICROGRAPHS OF THERMAL ANALYSIS SPECIMEN 2

a, b, and c Show Oxide Network; d is Region Free of Oxide and Shows Dislocation Cell Structure; 50,000X.

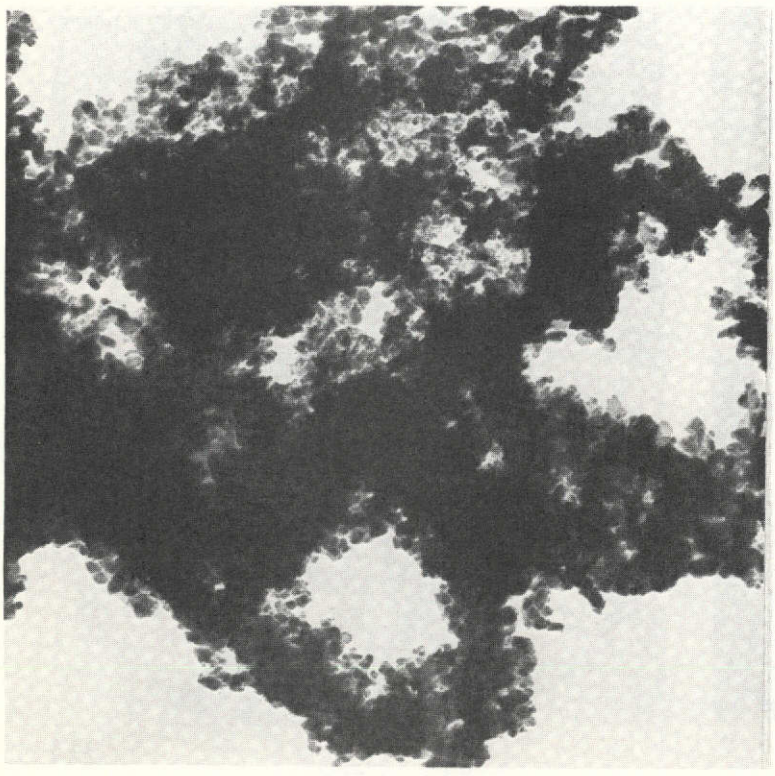

50,000X

2936

a.

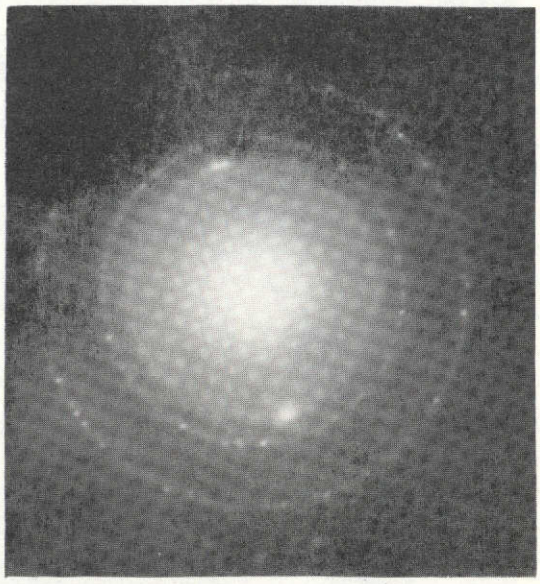

2935

b.

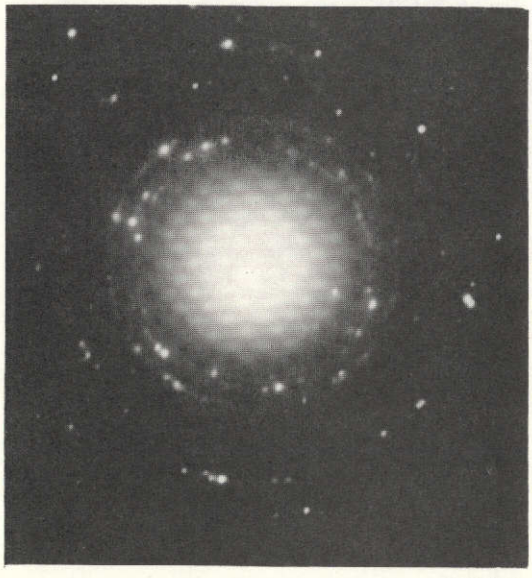

2969

c

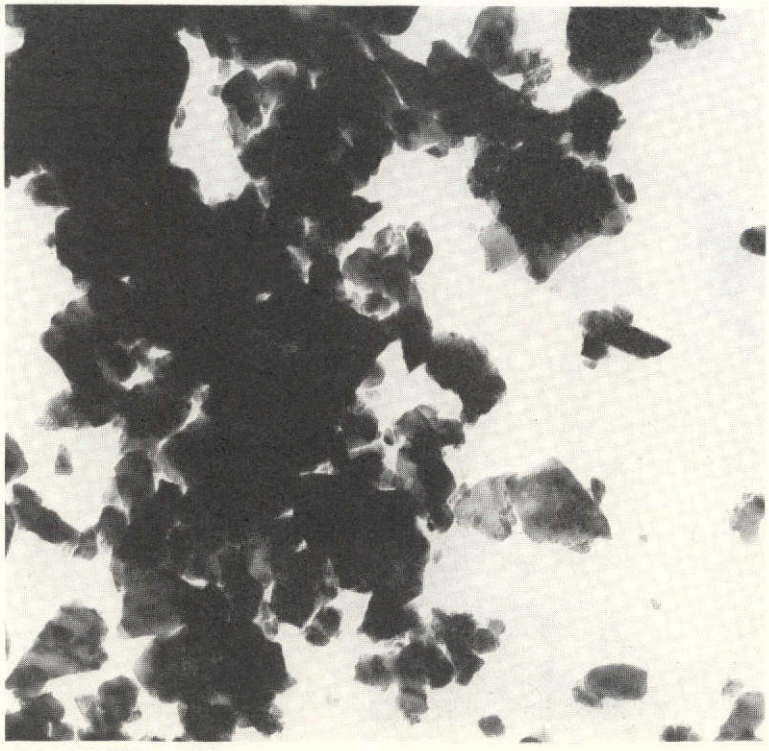

50,000X

2970

d.

FIGURE 8. TRANSMISSION ELECTRON MICROGRAPHS OF ALUMINUM OXIDE PRESENT IN THERMAL ANALYSIS SAMPLE 2(a) AND IN AS-RECEIVED SUPERGROUND Al_2O_3 (d)

B and c are SAD Patterns Corresponding to a and d, respectively.

corresponding selected area diffraction pattern, indexed as γ - Al_2O_3, is shown in Figure 8b. An electron micrograph of the ALCOA superground Al_2O_3 powder is shown in Figure 8d for reference. It is appreciably coarser than the naturally occurring oxide of Figure 8a. The selected area diffraction pattern corresponding to Figure 8d is shown in Figure 8c and has been indexed as α - Al_2O_3.

Scanning electron microscopy (SEM) has also been applied to the study of the oxide distribution and morphology. Metallographically polished and etched thermal analysis Samples 4, 5, and 17 were examined and showed that particulate matter attributed to Al_2O_3 was present in regions which corresponded to the fine network present in the optical photomicrographs. (See Figure 5 for example.) SEM micrographs of thermal analysis Sample 17 (Material 2, Condition T_2S) are shown in Figure 9. Figure 9a shows a relatively low magnification overview of a region containing some of the fine network structures. Figures 9b and 9c are higher magnification views of the fine structure showing the oxide particles. The two sizes of particles shown in Figure 9b probably correspond to the fine naturally occurring oxide and the coarser ALCOA unground Al_2O_3 which was added to the aluminum powder.

Discussion

Although some interesting observations were made on the melting, solidification, and structural characteristics of melted and solidified Al-Al_2O_3 powder compacts and the starting powders, it became obvious during our experimentation that the presence of Al_2O_3 in the size and concentration ranges investigated had no effect in promoting a fine-grain structure.

Accordingly, all further work on the Al-Al_2O_3 system was stopped, and our efforts were concentrated on attaining a fine-grain, ingot beryllium.

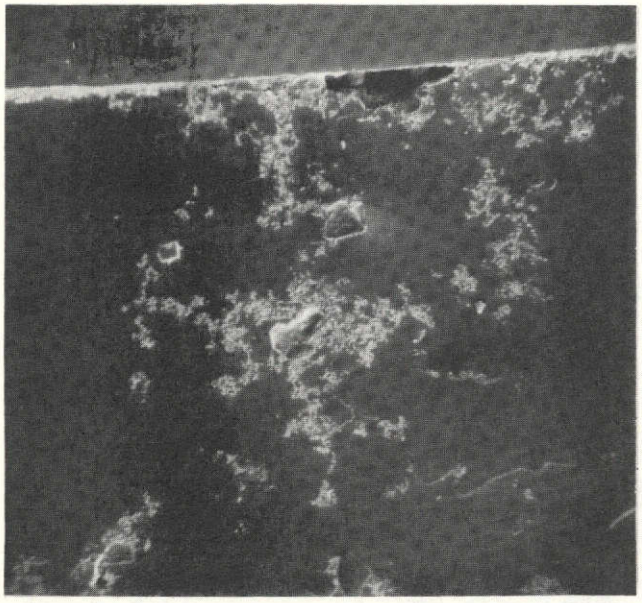

120X 393

a.

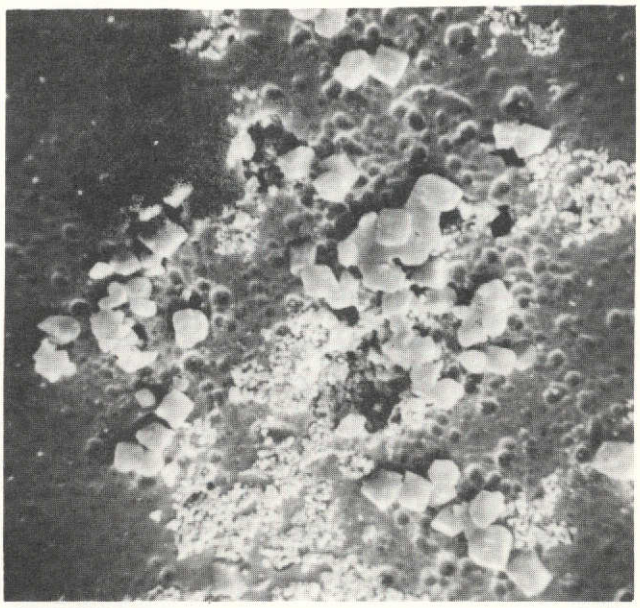

2000X 389

b.

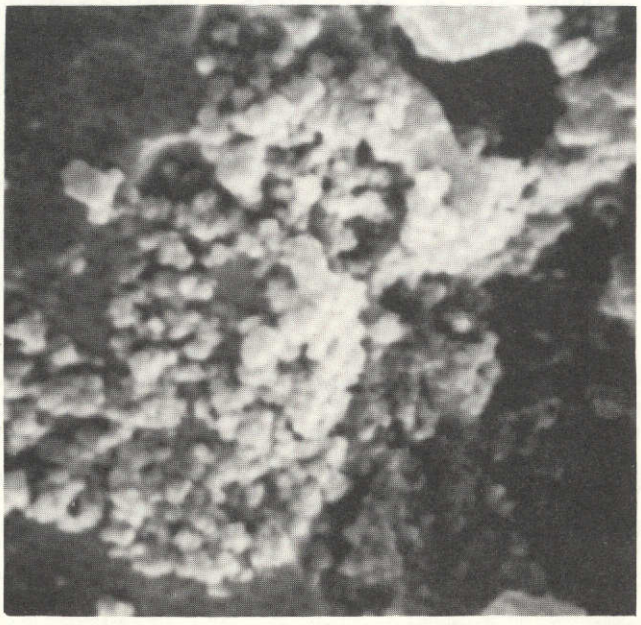

10,000X 392

c.

FIGURE 9. SEM MICROGRAPHS OF THERMAL ANALYSIS SPECIMEN 17

Polished Sections Etched in 20 Percent NaOH

Beryllium-Beryllium Oxide Experiments

Melting Experiments

With the aluminum-aluminum oxide investigation as background, simplified melting experiments were conducted on beryllium powder compacts with and without beryllium oxide powder in addition to the naturally occurring beryllium oxide existing on the powder particle surfaces. Compacts were made from high-purity -325 mesh P-1 beryllium powder obtained from Kawecki Berylco Industries (KBI) and from blends of the P-1 powder and -325 mesh high-purity BeO powder obtained from Brush Wellman. Some compacts were also made from a commercially pure -200 mesh beryllium powder (GB-2) also obtained from KBI. Analyses of these materials are presented in Tables 8 and 9. It should be noted that the BeO content of the P-1 beryllium powder (0.43 wt %) is significantly lower than the GB-2 powder (1.65 wt %).

Specimens for the melting experiments were prepared by cold isostatic pressing of the beryllium powder or blend of beryllium and BeO powders at 689 MPa (100 ksi) into a cylinder $\sim$ 1 cm in diameter x 5 cm long. Specimens 0.87-cm diameter x 0.83 cm long were machined from the compacts. The sample contained in a BeO crucible was rapidly heated and cooled in a small furnace specially constructed in an NRC vacuum evaporation system. The furnace is schematically shown in Figure 10. The specimen was usually outgassed in this equipment by preheating to $\sim$ 1000 C in a vacuum of 5×10^{-6} Torr and allowing it to cool before proceeding with the melting.

The furnace consists of a free-standing tantalum coil resistance heating element surrounding the BeO crucible containing the powder compact. The crucible is supported by an alumina tube having a central Pt - 10 wt % Rh thermocouple in contact with the base of the BeO crucible. The coil, crucible, and support are entirely surrounded by a series of tantalum radiation shields.

TABLE 8. KBI-SUPPLIED ANALYSIS OF BERYLLIUM POWDERS USED IN THE PRESENT INVESTIGATION

Impurity	Level, ppm by weight	
	-200 Mesh, Type GB-2	-325 Mesh, Type P-1
BeO	16,500	4,300
Fe	1,660	140
C	1,260	300
Al	430	61
Mg	270	32
Si	540	61
Ni	170	6
Mn	60	17
Cr	75	6
Ca	<200	--
Co	10	<5
Cu	75	40
Sn	<100	--
Ag	10	--
Pb	1	<1
Mo	<10	<10
Zn	<100	--

TABLE 9. IMPURITY ANALYSES FOR TYPE UOX BeO POWDER--BRUSH WELLMAN COMPANY

Element	Content in ppm by Weight	
	Typical	Maximum
S	800	1500
Al	40	100
Ca	<30	50
Fe	20	50
Mg	25	50
Si	50	100
Na	25	50
B	<1	3
Cd	<1	2
Cr	5	10
Co	<1	3
Cu	<2	5
Pb	<2	5
Li	<1	3
Mn	2	5
Mo	<3	5
Ni	3	10
Ag	<1	3

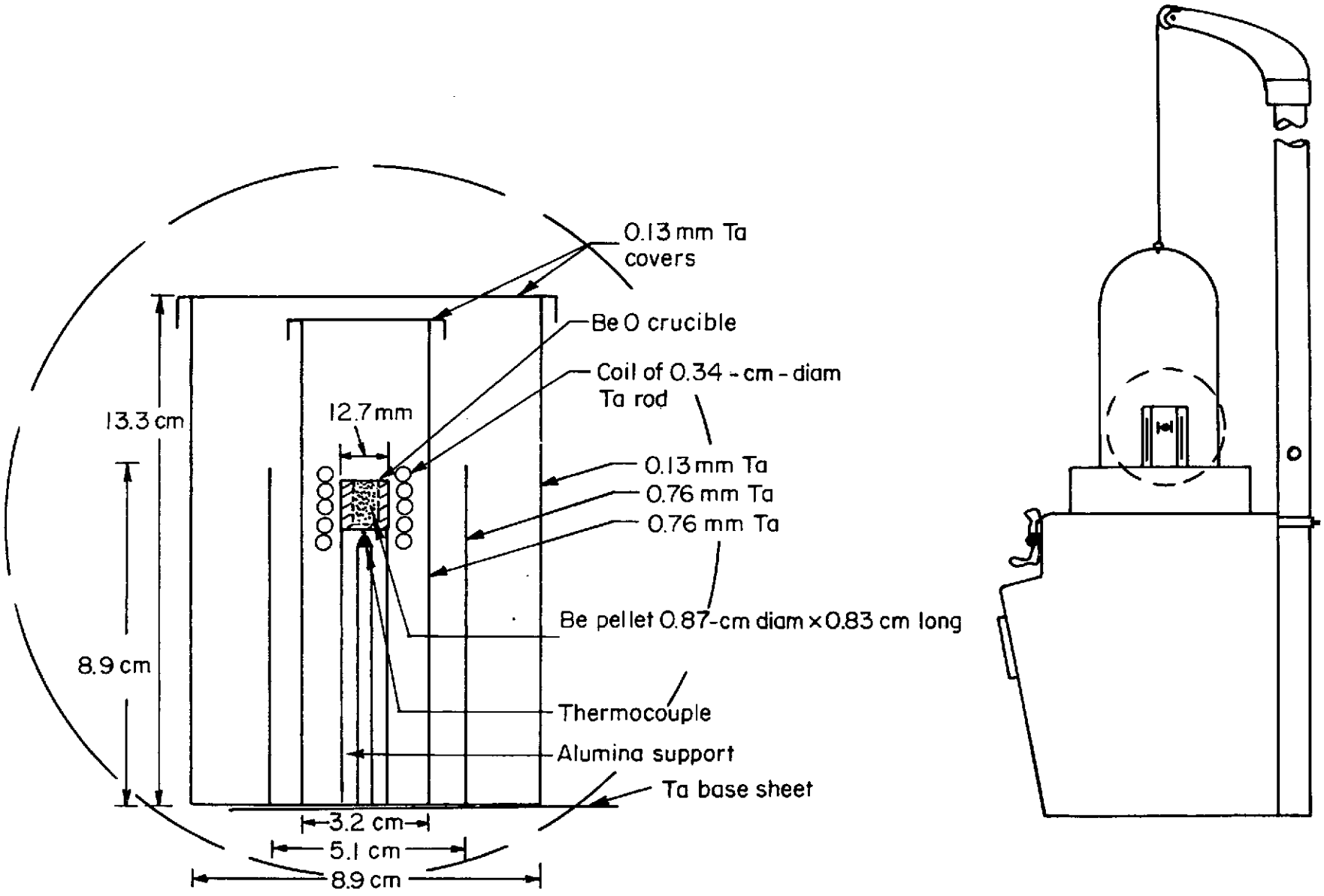

FIGURE 10. SCHEMATIC DRAWING OF TANTALUM RESISTANCE FURNACE USED IN THE BERYLLIUM MELTING AND GRAIN-GROWTH EXPERIMENTS

Three successful melting experiments were run in this series. In the first (Be Melt 1), a P-1 powder compact was melted by heating to 1404 C and allowed to cool at a measured average rate of 2.3 C through the solidification temperature. Approximately 500 watts (5 v and 100 amp) was needed to melt the sample. Although the arrangement of the thermocouple in the melting apparatus was not designed to provide heating and cooling curves which could sensitively detect the thermal arrests on melting and solidification, a small heat effect was seen on solidification.

Metallographic examination of a longitudinal section of the melted and solidified billet revealed a structure which consisted of very large grains and a fine distribution of pores. There was no obvious concentration of oxide as had been seen in the Al-Al_2O_3 system nor any fine-grain regions.

The second melt was made with a GB-2 powder compact (Be Melt 4). This experiment was conducted in order to determine whether the higher oxide content present in this material would lead to a finer grain structure. The compact was initially outgassed by heating to 1050 C in approximately 10 minutes and furnace cooled to room temperature. The sample was subsequently melted at an indicated temperature at the crucible base of 1425 C. Approximately 6 v and 120 amp were required for the melting. An average cooling rate through the solidification range was approximately 3.5 C per sec.

A polished longitudinal section of the billet was subsequently examined with the results shown in Figure 11. The bright-light macrograph of Figure 11a reveals a structure containing a fairly uniform distribution of fine pores throughout most of the billet except for a solid skin. Figures 11b, c, and d show the grain structure as revealed by polarized light observation. In all cases the grain size is extremely large. Isolated finer grains are sometimes seen. Even these, however, are relatively large compared to those obtained in commercial powder metallurgy material.

The third melting experiment (Be Melt 5) was conducted with a compact of P-1 beryllium powder blended with 5 vol % UOX BeO powder. The

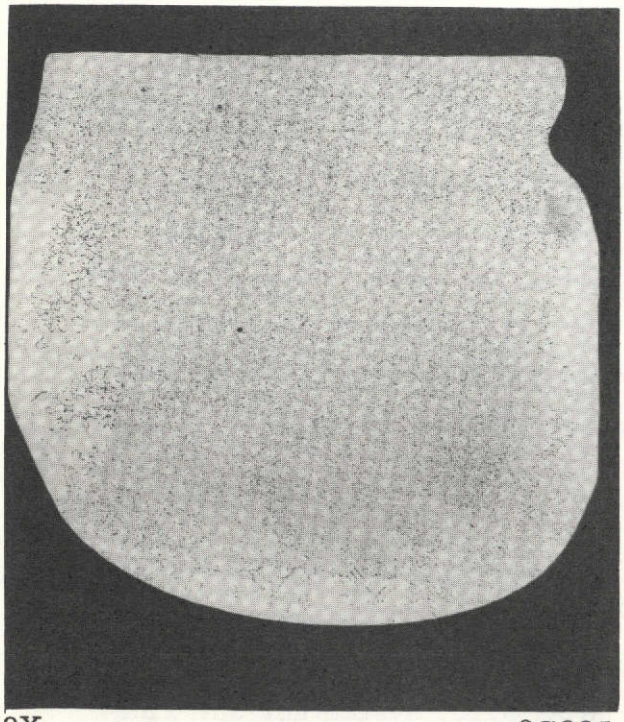

9X 8G885

a. Bright Light

50X 8G888

b. Polarized Light

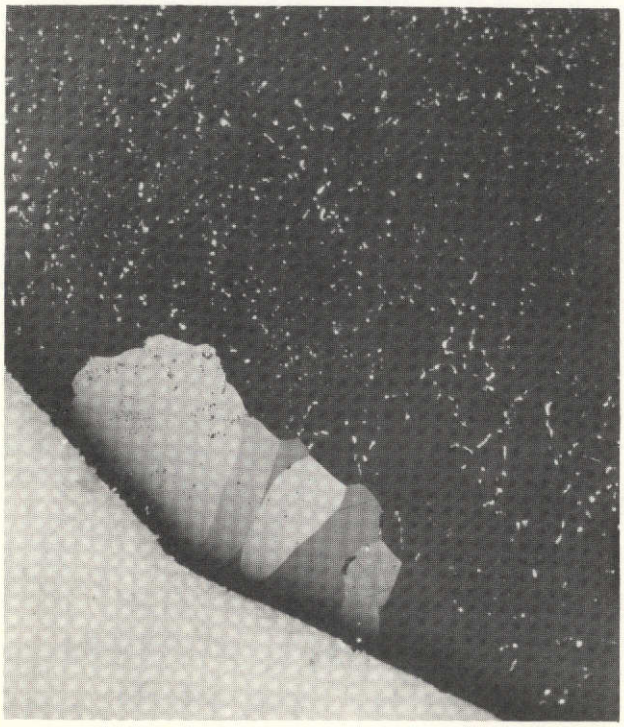

50X 8G886

c. Polarized Light

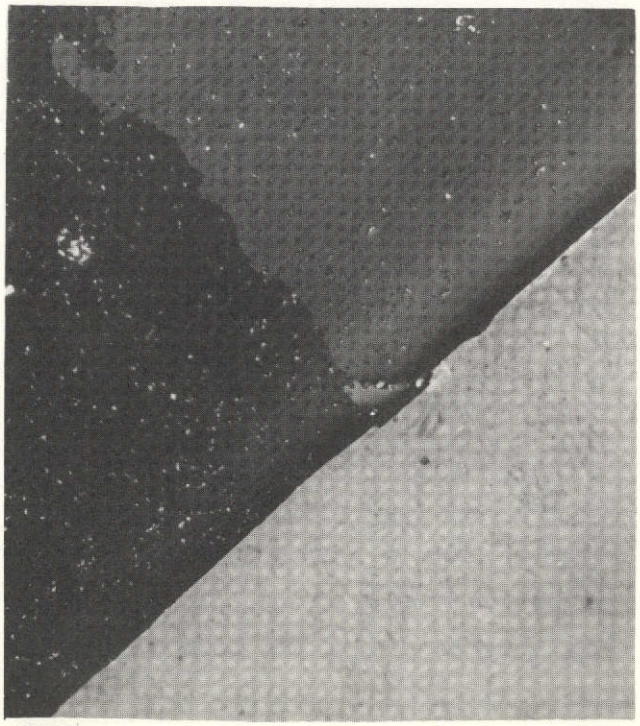

50X 8G887

d. Polarized Light

FIGURE 11. MICROSTRUCTURES OF LONGITUDINAL SECTION OF Be MELT 4

sample was outgassed at 1020 C and melted at a temperature 1422 C as indicated at the bottom of the BeO crucible. A power level of 120 amp at 60 v was more than adequate to perform the melting. The sample was heated to temperature in ∿ 4 minutes and the power cut off. An average cooling rate of 4.7 C per sec was measured.

A longitudinal section of the solidified billet was examined metallographically, revealing the microstructures presented in Figure 12. Examination in bright light (Figures 12b and d) shows a rather fine network of oxide surrounding metal which appears to be fine grained. Further examination in polarized light, however, reveals that only part of the compact has melted and that very large columnar grains are present in the melted region (Figure 12c), while the fine structure typical of a powder metallurgy product is present in the unmelted region (Figure 12a). The interfacial zone between the melted and unmelted regions is revealed in Figure 12e.

These results indicate that even though there is a fine network of BeO fairly uniformly distributed through the melted material, it either does not contribute to nucleation or if it does contribute, rapid grain growth unhampered by the oxide network eliminates the fine nucleated grains.

Characteristics of BeO in Melted Be-BeO Compacts

Transmission electron microscopy and selected area electron diffraction were carried out on samples of Beryllium Melt No. 4 (commercially pure Be containing 1.65 wt % BeO) in order to more closely examine the BeO network and confirm that the particle network observed did indeed consist of BeO. Samples for electron microscopic observation were prepared by cutting a nominally 1-mm-thick slice from the billet with a water-cooled cut-off wheel and mechanically polishing to ∿ 0.2 mm on fine abrasive paper. 3-mm-diameter discs were then punched and final polishing performed in a Fishione Twin Jet Electropolishing Unit at a temperature of 10 to 15 C and at 32 v. A solution consisting of 400 ml ethylene glycol, 40 ml HNO_3, 8 ml H_2SO_4, and 8 ml HCl was used as the electrolyte.

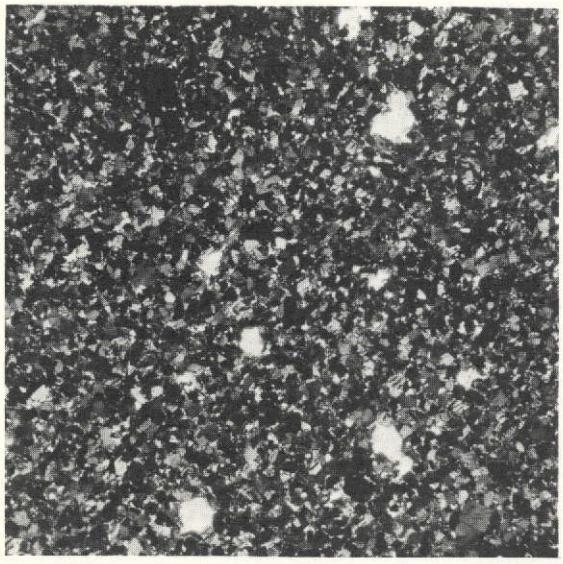

OH203

a.

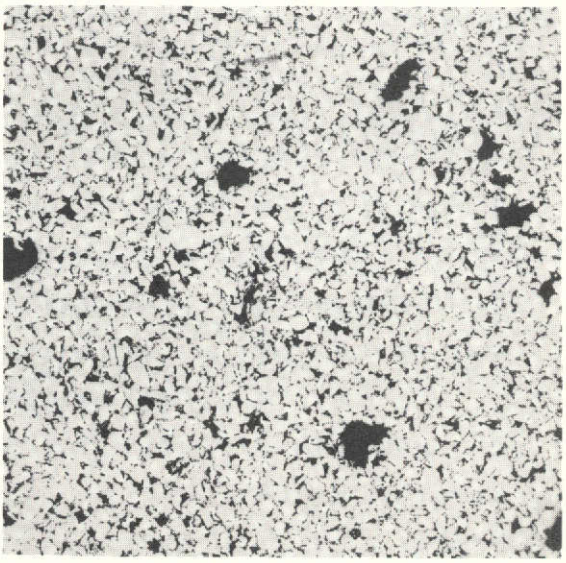

OH202

b.

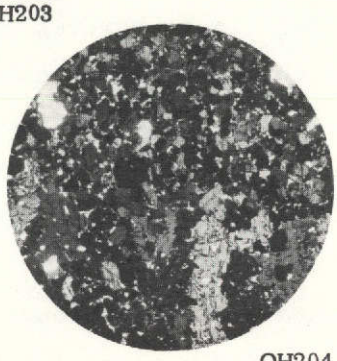

e. OH204

OH205

c.

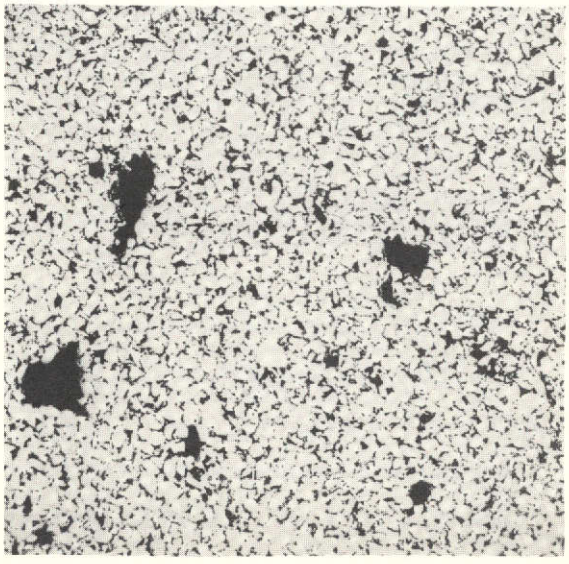

OH201

d.

FIGURE 12. MICROSTRUCTURES OF LONGITUDINAL SECTION OF SAMPLE Be MELT 5

Figures a and b are, respectively, polarized- and bright-light views of unmelted area; c and d are corresponding views in the melted region. Figure e is a polarized-light micrograph of the interfacial area between unmelted and melted regions. (50X)

The TEM observations (Figure 13) revealed the presence of a network of particles ranging in diameter from 0.06 to 0.5 μ. Where selected area diffraction patterns have been taken, the particulate matter has been identified as BeO.

Grain-Growth Studies

Introduction. Since the melting experiments previously described did not produce a fine grain size in any of the processed specimens, it was decided that a series of experiments would be carried out to determine whether grain growth in the solid beryllium at temperatures near the melting point was contributing to the coarse grain size observed in the melted samples. Accordingly, a series of grain-growth experiments were conducted on unmelted powder compacts either in the cold-pressed or cold and hot isostatically pressed condition. At the time of the experiments it was reasoned that if no appreciable growth growth was observed, the large ingot grain size could then be attributed to a nucleation problem. However, it was not appreciated at that time that the grain-growth characteristics of an unmelted material can possibly be appreciably different from those of melted and solidified material. This aspect of the problem is discussed in a later section.

Experimental. The material used was either cold or hot isostatically pressed P-1 beryllium powder containing a dispersion of beryllium oxide resulting from the naturally occurring oxide on the powder surfaces. Three beryllium powder compacts 1.6 cm in diameter by 12.5 cm long were prepared by cold isostatic pressing (CIP) at 689 MPa (100,000 psi). One CIP rod was hot isostatically pressed (HIP) at 930 C for 3 hours. Samples were machined to 0.95-cm diameter and cut to a length of 0.95 cm. A thermocouple well 0.38 cm in diameter by 0.48 cm deep was machined into each sample base. Although no density measurements were made, from past experience CIP samples are expected to be ∿ 85 percent dense and the CIP/HIP samples fully dense.

The samples (Be GS-1 through Be GS-5) were outgassed and subjected to thermal exposures in the bell jar vacuum furnace used in the

7500X 3001

a.

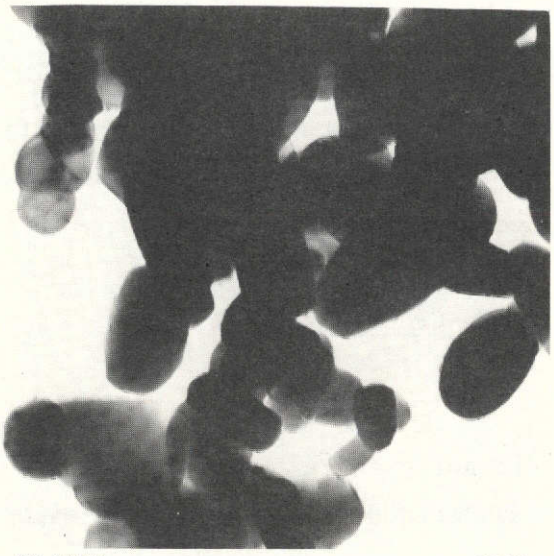

50,000X 2955

b.

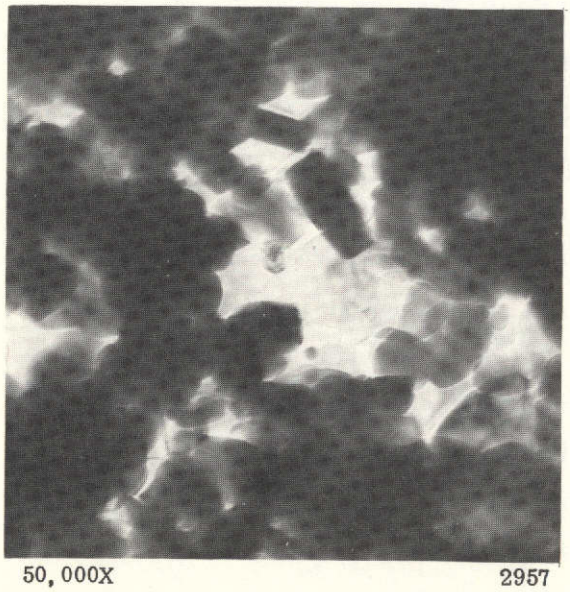

50,000X 2957

c.

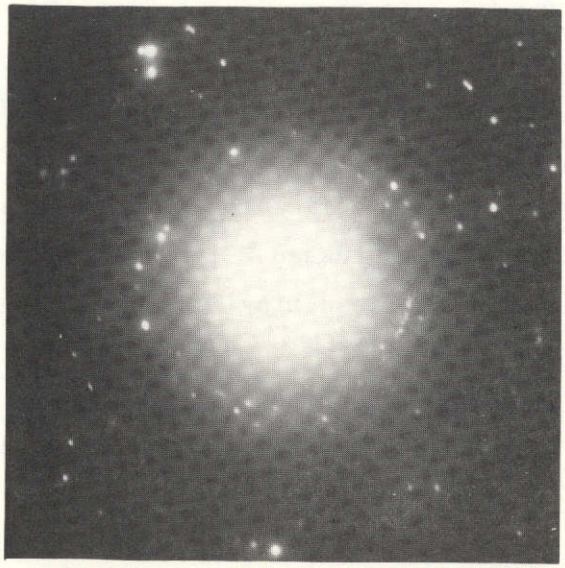

2958

d.

FIGURE 13. TRANSMISSION ELECTRON PHOTOMICROGRAPHS OF BeO NETWORK IN MELTED BERYLLIUM POWDER COMPACT 4

Figure d shows that SAD pattern corresponding to particles in Figure c.

previous melting experiments (see Figure 10). The samples were supported directly by a thermocouple inserted into the thermocouple well. No beryllium oxide (BeO) crucible was used. A continuous record of temperature was obtained for each of these experiments. The treatment conditions, viz, outgassing temperature, maximum temperature, and time at temperature above 1250 C for various samples, are given in Table 10 and include specimens treated in the HCP α-Be phase field (below 1260 C) and in the BCC β-Be phase field just below the melting point of beryllium (1283 C).

Metallographic examination of the samples delineated in Table 10 revealed the microstructures shown in Figures 14 and 15. The photomicrographs in Figure 14 are arranged in order of increasing exposure temperature and show that grain growth in the α phase (Figure 14a) or in the β phase (Figures 14b-14d, and 15a and 15b) is not significant. It should also be noted that the finest grain structure is obtained in the HIP material (Be GS-2, Figure 14b). This effect could be due to recrystallization during heating or cooling or due to the absence of vacancy sources in the form of pores which are present in the CIP samples. The presence of these pores could lead to enhanced diffusion and grain growth.

Some of the photomicrographs of Figure 15 (Specimen Be GS-3) show evidence of partial melting as expected from the indicated treatment temperature of 1286 C. The bottom melted region (Figure 15c) shows the large columnar grains typical of ingot beryllium. Figure 15a shows the fine-grain structure of the unmelted top region; and Figure 15b, the interfacial region between the melted and unmelted portions.

Discussion. From examination of the structures in Figures 14 and 15, it can be concluded that

(1) Melting occurred at temperatures close to 1286 C in agreement with the published melting point of beryllium (1283 C).

(2) No significant grain growth occurs in the HCP α phase or the BCC β phase at temperatures approaching the melting point of beryllium.

The second conclusion is certainly valid for unmelted beryllium powder metallurgy products, both CIP or CIP and HIP. However, it is

TABLE 10. THERMAL EXPOSURE FOR Be GRAIN-GROWTH EXPERIMENTS

Sample No.	Outgassing Temp, C	Max Temp, C	Time, minutes at temp above 1250 C
BeGS-1 (CIP)	1062	1255	14
BeGS-2 (CIP/HIP)	1051	1266	9
BeGS-3 (CIP)	1051	1286	10.5
BeGS-4 (CIP)	1052	1280	1.5
BeGS-5 (CIP)	1051	1277	7.25

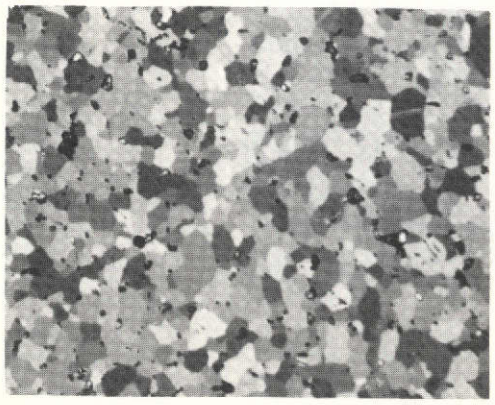

OH334

a. Be GS-1
1255 C Maximum Temperature

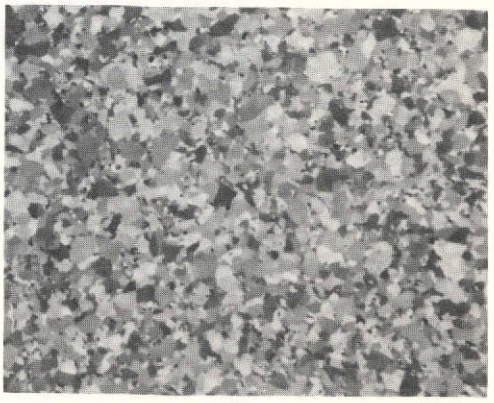

OH335

b. Be GS-2
1266 C Maximum Temperature
(CIP/HIP-930 C Maximum
Temperature – 3 Hours)

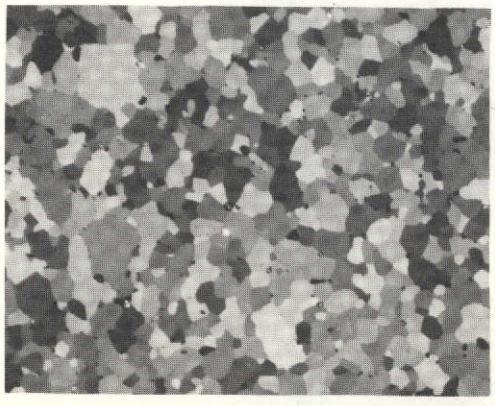

OH340

c. Be GS-5
1277 C Maximum Temperature

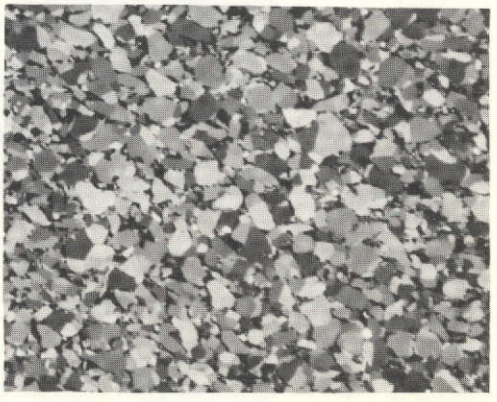

OH339

d. Be GS-4
1280 C Maximum Temperature

FIGURE 14. PHOTOMICROGRAPHS OF BERYLLIUM GRAIN-GROWTH SPECIMENS (100X)

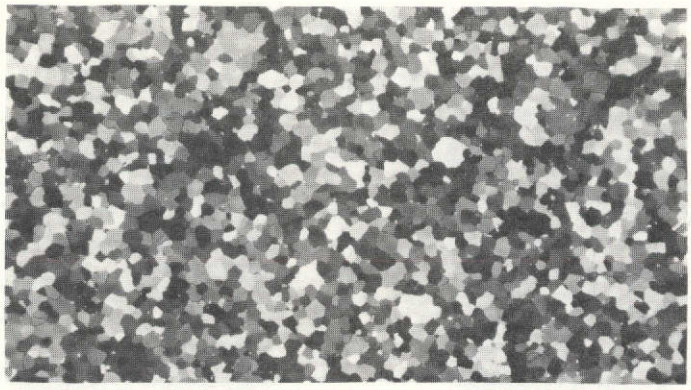

50X OH336

a. Unmelted (Top) Region

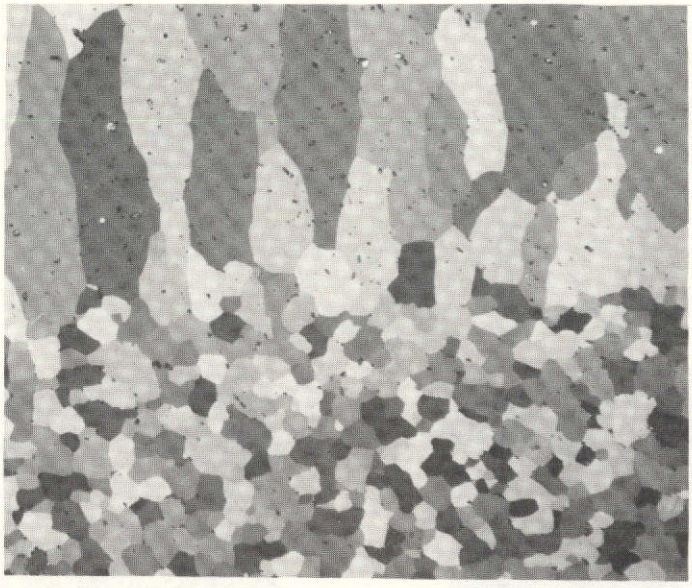

100X OH337

b. Interfacial Zone

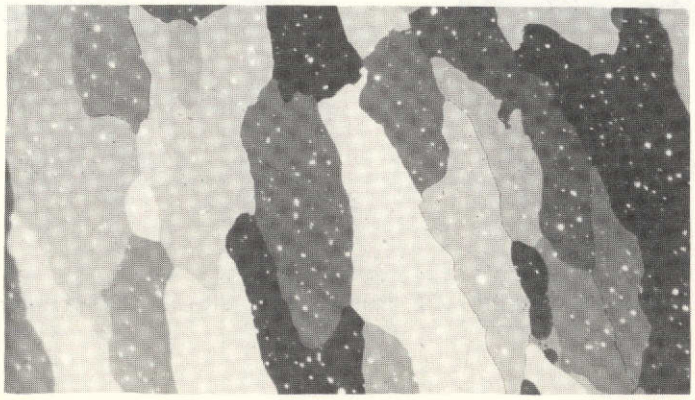

100X OH338

c. Melted (Bottom) Region

FIGURE 15. PHOTOMICROGRAPHS OF Be GS-3 (1286 C MAXIMUM TEMPERATURE)

possible that melting the powder compact leads to agglomeration of the fine beryllium oxide delineating the original powder particles. Beryllium oxide has been found to be an effective grain-growth inhibitor when it is extremely fine (∿ 400 A). It becomes ineffective, however, when it coarsens much beyond that size[1].

With the realization that there was not appreciable grain growth in unmelted beryllium, there were two outstanding questions that required answers.

(1) Is the coarse grain structure in the melted beryllium powder compacts due to rapid grain growth in the solidified material, or

(2) Is it due to a lack of agents for heterogeneous nucleation of a fine-grain solid from the molten beryllium containing beryllium oxide?

The remainder of the program was devoted to conducting experiments which would help provide answers to these questions.

To provide information for answering the first question, we have conducted a comparative study on the size and distribution of the beryllium oxide in unmelted and melted beryllium-beryllium oxide powder compacts.

To determine whether there is a deficiency in effective heterogeneous nuclei, a limited study has been conducted in which other potential nucleating agents (inoculants) were blended with the beryllium powder and the blended powder compacted, melted, and the solidified metal examined to determine whether the inoculant was effective. If success were achieved in this part of the investigation, it could be concluded that the problem in achieving a fine-grain beryllium casting, even with the addition of BeO, is associated with the lack of effective nucleating agents.

Evaluation of Candidate Nucleating Agents

In addition to BeO which has already been examined, ten other potential nucleating agents were selected on the basis of their estimated

stability in molten beryllium and considerations of lattice match with the nucleated solid β beryllium. Interfacial energy considerations referred to in the Background Section of this report could not be applied because of a complete absence of the required data. These agents are listed in Table 11. Using the blending, compacting, and melting procedures developed for the beryllium-beryllium oxide experiments, samples representing the compositions listed in Table 11 were melted, sectioned, and examined metallographically.

The initial set of samples which were heated to maximum temperatures between 1384 and 1475 C as indicated at the base of the BeO crucible* contained 2 vol % additions of TaN, TiB_2, Ge, WC, and BN. The microstructures of this group are shown in Figure 16 and generally consist of coarse grains. Some relatively fine-grained areas were observed in the Be-Ge compact, Figure 16c; and in the WC compact, Figure 16d. In one of the experiments with the BN additions, thermocouple failure at an indicated temperature of 1384 C ended the experiment. As shown in Figure 16e, no evidence of melting was observed. A repeat of the BN experiment at 1450 C produced the extremely coarse grain structure shown in Figure 16f.

In the light of the somewhat encouraging results obtained with the 2 vol % additions of Ge and WC, additional experiments were conducted with 5 vol % additions of these potential grain refiners. Also, five other potential inoculants at the 2 vol % concentration were explored at this time.

- CrB_2
- TiO_2
- Cr_3C_2
- VC
- Mo_2C.

The samples in this series were all heated to an indicated temperature of 1450 C. Three of the samples (2 vol % Mo_2C, 5 vol % Ge, and 2 vol % Cr_3C_2)

---

* The indicated temperature is appreciably higher than the temperature in the sample due to the rapid heating rates used.

TABLE 11. ADDITIONS INVESTIGATED AS POTENTIAL GRAIN REFINERS OF INGOT BERYLLIUM

Additions	Source[a]	Purity[b]	Concentration, vol %
CrB_2	A	99.9	2
TiO_2	A	99.9	2
WC	B	99.8	2, 5
VC	A	99.9	2
TaN	B	99	2
TiB_2	B	99.8	2
Ge	B	99.999	2, 5
BN	B	99.7	2
Mo_2C	A	99.9	2
Cr_3C_2	A	99.8	2

(a) A--Atlantic Equipment Engineers, Bergenfield, New Jersey.

B--Alfa Inorganics, Beverly, Massachusetts.

(b) Vendor provided.

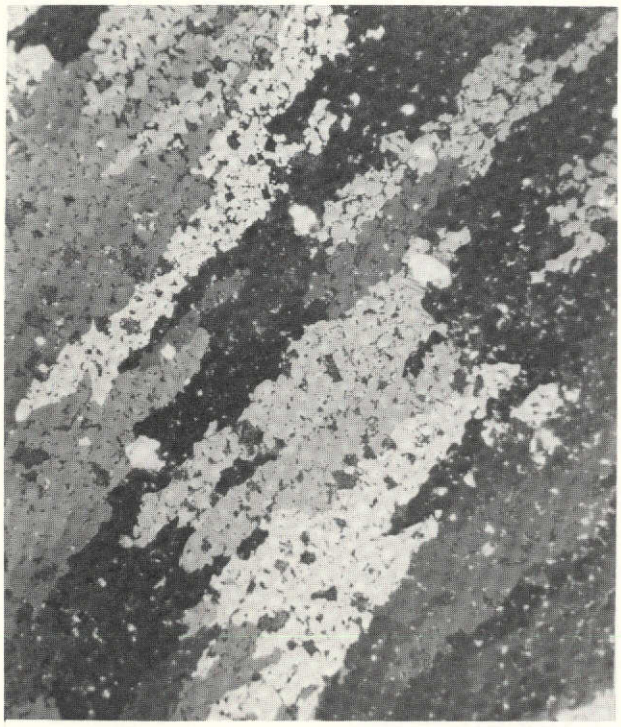

OH610

a. TaN

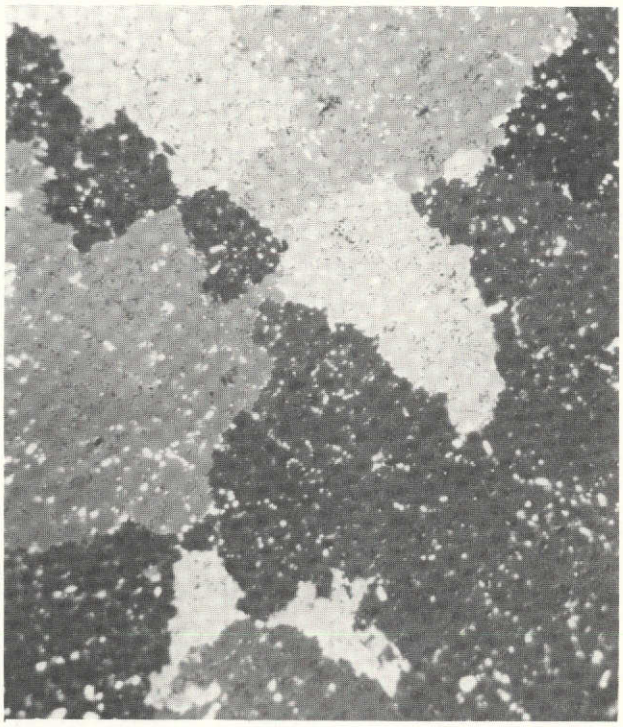

OH611

b. TiB_2

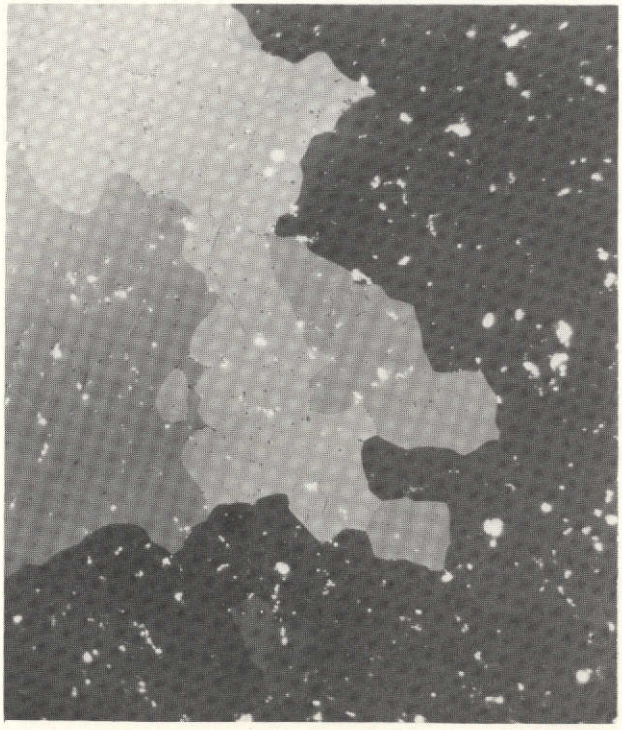

OH612

c. Ge

FIGURE 16. PHOTOMICROGRAPHS OF MELTED BERYLLIUM POWDER COMPACTS 2 VOLUME PERCENT OF THE INDICATED INOCULANTS (50X)

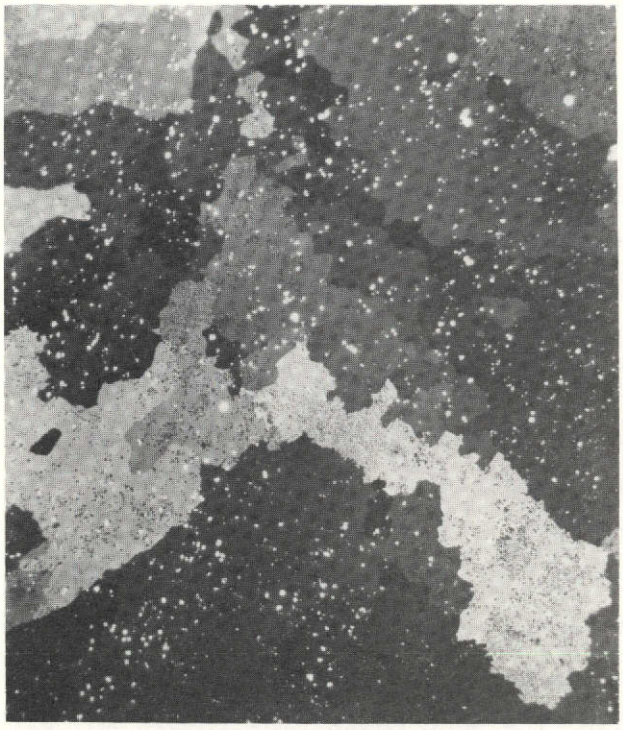

OH613

d. WC

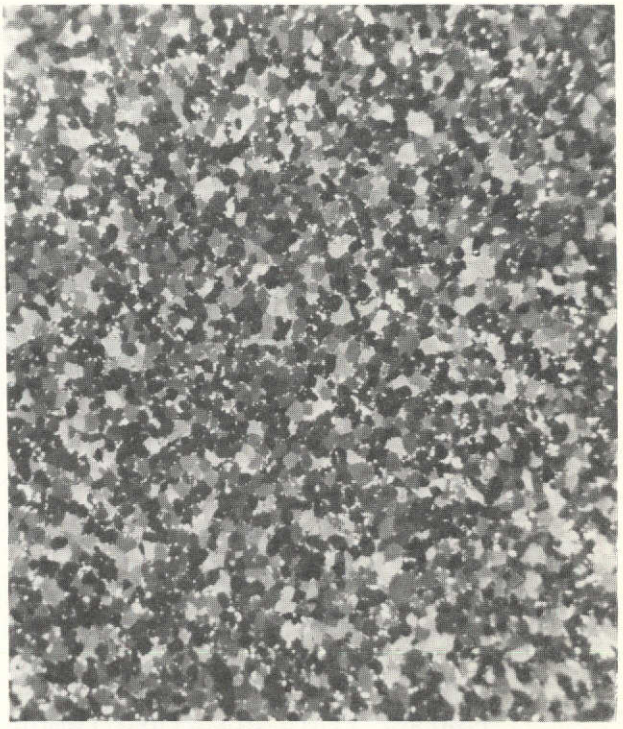

OH614

e. Unmelted BN

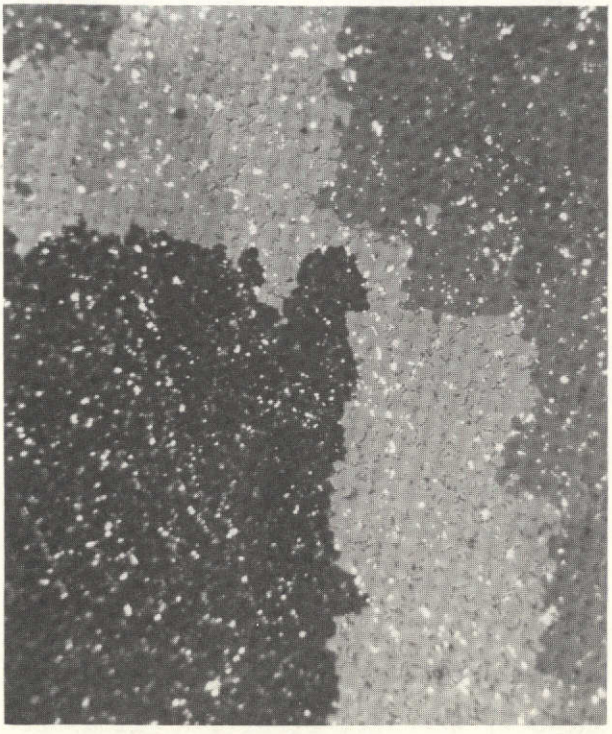

OH615

f. BN

FIGURE 16. (CONTINUED)

in this series were completely unmelted. Photomicrographs of the rest of the samples which had either completely or partially melted are presented in Figure 17 and in all cases exhibited coarse grain structures.

Melting experiments were rerun at 1500 C on the three samples which had not melted in the previous experimental series. Photomicrographs of these samples are presented in Figures 18a-c and show that the fine grain size present in the unmelted powder metallurgy compact is generally replaced with a coarse grain structure. There are regions, however, in Figures 18a (Mo_2C) and 18c (Cr_3C_2) where there are finer grain areas. In the case of the Cr_3C_2 addition of Figure 18c, this appears to be a case of incomplete melting. A second compact of the same composition heated to 1550 C, approximately 50 C higher than that of 1c, shows a much coarser grain structure (Figure 18d). The Mo_2C containing sample may also behave in the same manner when heated to a higher temperature. Additional work is required to check out this point.

With the possible exception of the Mo_2C additions just referred to, none of the additions (see Table 11) to the P-1 beryllium compacts which we have investigated has produced the desired grain refinement characteristics. Since none of the potential grain refinement agents was found to be effective, no conclusions can be made regarding the relative roles of nucleation of the solid and grain growth in the solidified metal.

Characteristics of BeO in Melted Compacts of P-1 Beryllium

Although this study has established that grain growth in an unmelted powder compact is negligible even in specimens heated to temperatures within a few degrees of the melting point for exposure times of a few minutes, there is a distinct possibility that once melting has occurred, the grain-growth inhibition provided by the naturally occurring BeO is removed. As shown by Webster, et al.,[1] it is necessary to have a fine oxide present to avoid grain growth in a beryllium powder metallurgy product. Grain growth is usually accompanied by the agglomeration of the

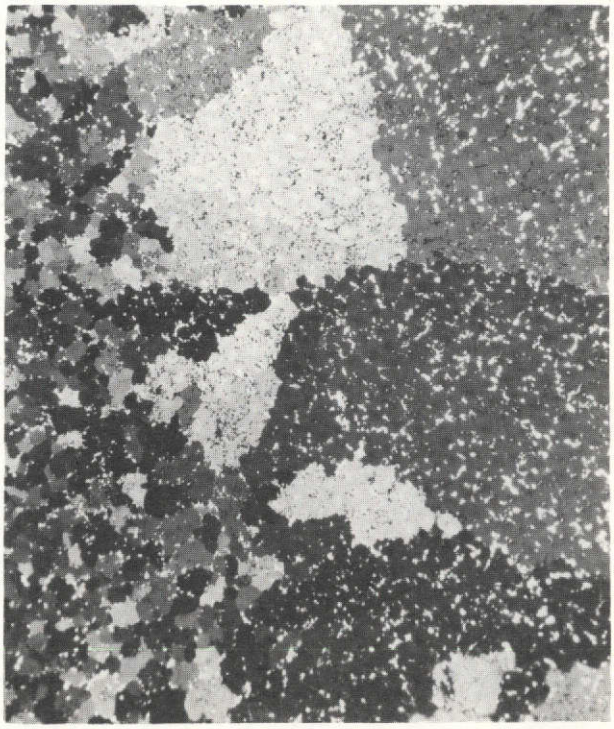

2H000

a. 2 Vol% CrB_2

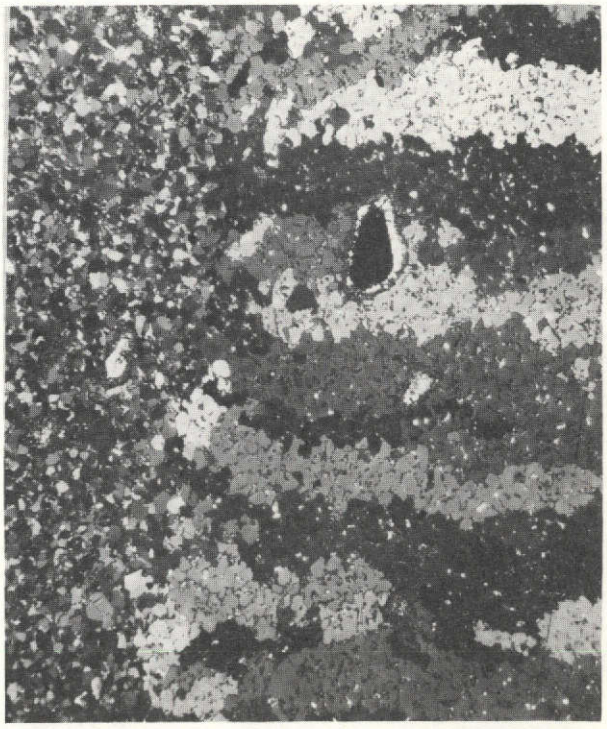

2H004

b. 2 Vol% TiO_2

2H005

c. 5 Vol% WC

2H001

d. 2 Vol% VC

FIGURE 17. PHOTOMICROGRAPHS OF MELTED AND PARTIALLY MELTED BERYLLIUM COMPACTS CONTAINING THE INDICATED ADDITIONS (50X POLARIZED LIGHT)

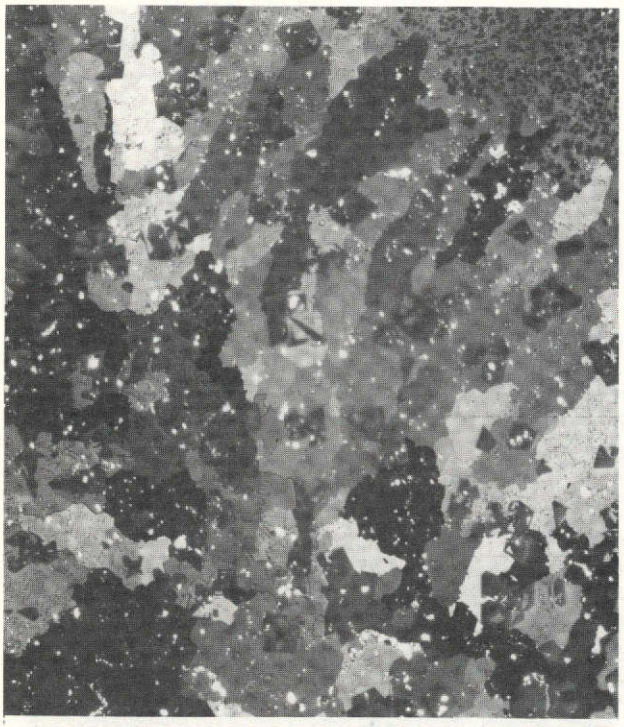

a. 2 Vol % Mo_2C

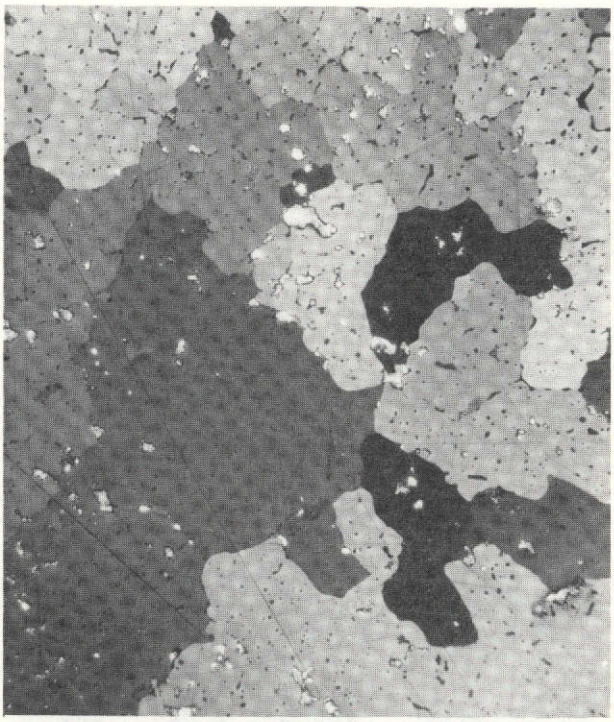

b. 5 Vol % Ge

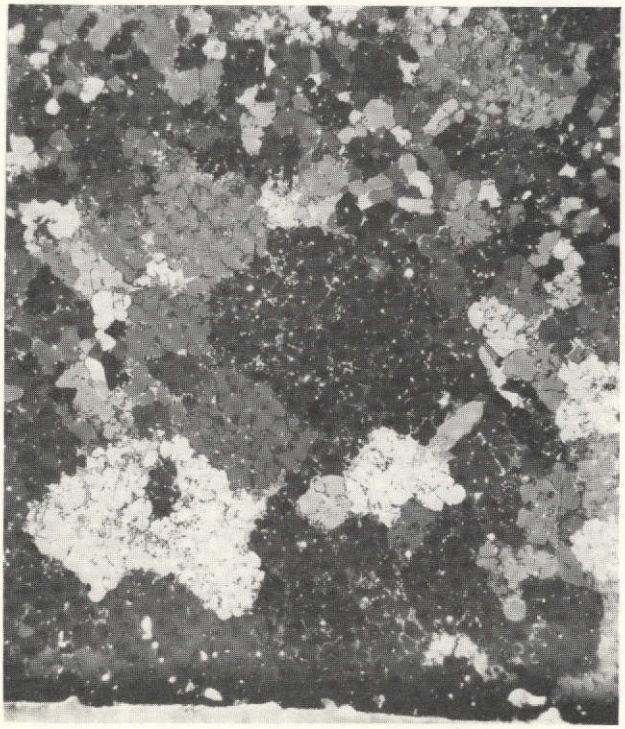

c. 2 Vol % Cr_3C_2

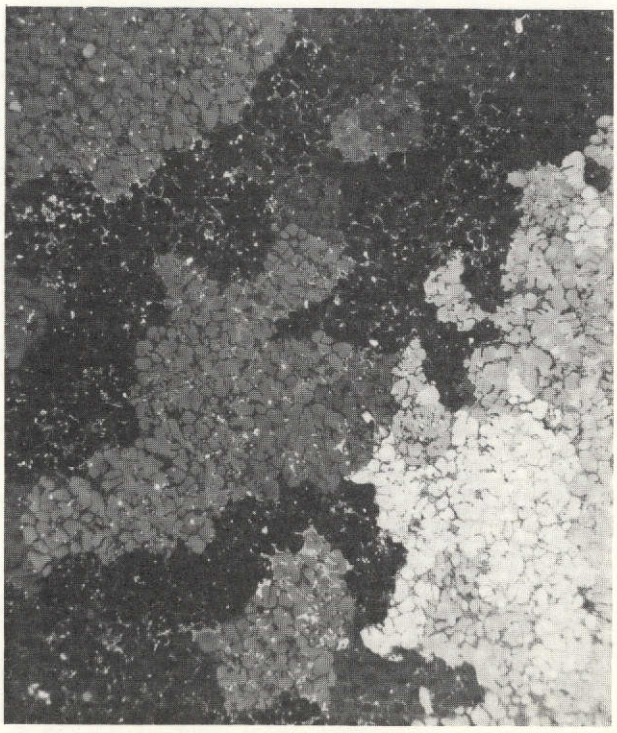

d. 2 Vol % Cr_3C_2

FIGURE 18. PHOTOMICROGRAPHS OF MELTED AND SOLIDIFIED POWDER COMPACTS OF P-1 BERYLLIUM WITH INDICATED ADDITIONS

D is a repeat of c at a higher temperature

beryllium oxide. As discussed in the Background Section of this report, the presence of a liquid phase should accelerate agglomeration of the oxide, thus removing the grain-growth inhibition. It was reasoned that the presence of a liquid phase could allow oxide agglomeration to take place by Stokes settling and convection current induced collisions. These mechanisms are being analyzed in another MSFC program.[2]

Transmission electron microscopy was used to determine the oxide distribution in the melted and unmelted regions of Specimen Be GS-3 produced from P-1 powder.

Typical micrographs are presented in Figure 19 and reveal that although some agglomeration has occurred in the solid heated close to its melting temperature*, the degree of agglomerate formation is much greater in the melted region.

These observations thus support the possibility that the large grain (size) in the melted and solidified powder compact is caused by the agglomeration of the oxide during the melting operation. Since agglomeration is accelerated by collision processes caused by gravity-induced Stokes settling and convection currents, it is anticipated that processing beryllium-beryllium oxide powder compacts at 0 g would prevent the oxide agglomeration and the resultant destruction of its grain-growth inhibition. If nucleation is no problem, it should be then possible to produce a fine-grain ingot at 0 g.

DEFINITION OF LOW-G EXPERIMENTS

Introduction

Our grain-growth experiments in unmelted beryllium powder compacts have shown that the naturally occurring, finely divided oxide present on the beryllium-powder particles prevent rapid grain growth from occurring.

---

* Agglomeration of the oxide in the solid is thought to be due to localized grain boundary melting due to impurities such as Al, Si, and Mg.

3018

a. Melted Region

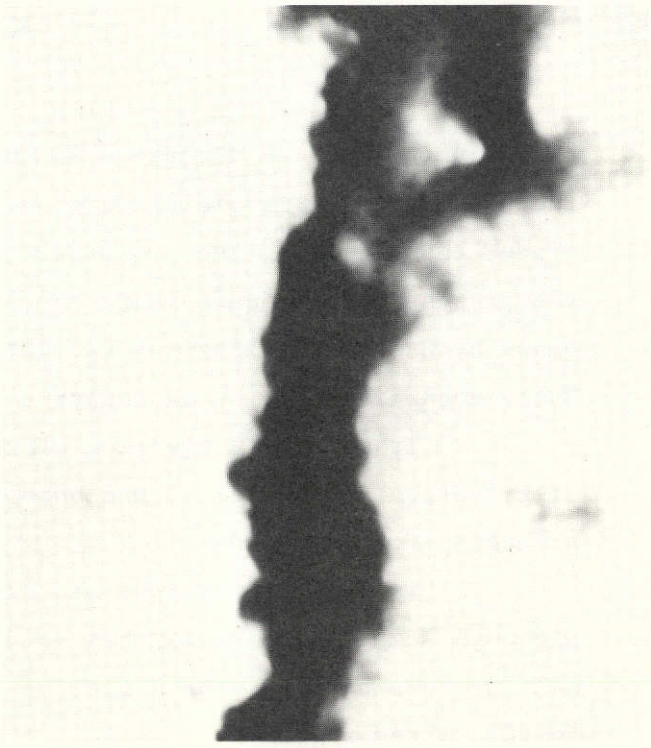

3019

b. Melted Region

3011

c. Unmelted Region

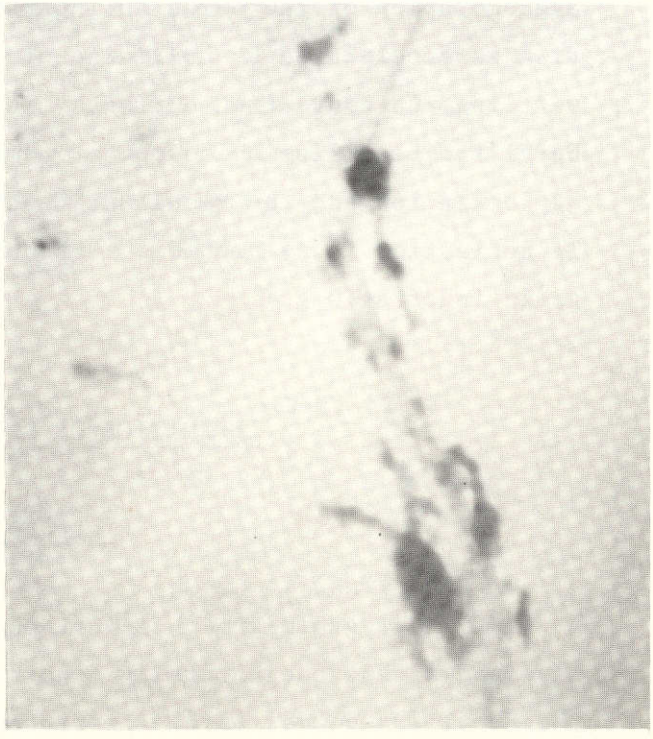

3012

d. Unmelted Region

FIGURE 19. TRANSMISSION ELECTRON MICROGRAPHS TAKEN OF SAMPLE Be GS-3 (10,000X)

Further experiments have shown that once the beryllium has been melted, the oxide tends to agglomerate. In this condition the oxide no longer acts as a grain-growth inhibitor.[1] Under such circumstances, a finely nucleated grain structure would be effectively masked by rapid grain growth.

Since a number of the more effective mechanisms causing agglomeration are due to collisions induced by gravity-driven flow processes,[2] melting and solidification at 0 g should help maintain a fine distribution of the naturally occurring oxide during the melting process. Likewise, the addition of other inoculants may prove to be more beneficial when done at 0 g, since they also would tend to remain more uniformly dispersed and, consequently, provide a relatively large number of nucleation sites. Their fine distribution would also tend to inhibit grain growth after solidification.

Accordingly, we are suggesting two basic low-g experiments; the first will be addressed to the conduct of meaningful melting experiments with beryllium powder compacts containing the naturally occurring oxide, and the second will be concerned with conducting similar experiments with the addition of potential nucleating agents.

If the first set of experiments provide positive grain refinement results and if the beryllium oxide remains unagglomerated during melting and solidification at low g, these results would support the hypothesis that grain refinement at 1 g was not achieved in the melting of beryllium powder compacts because the beryllium oxide present on the powder-particle surface agglomerates during the melting process and no longer acts as a grain-growth inhibitor.

Alternatively, if in the first series of low-g experiments grain refinement is not achieved but the beryllium oxide remains unagglomerated during the processing, it is more than likely that the problem in obtaining a fine-grain ingot beryllium is due to a deficiency in the number of heterogeneous nucleation sites. Lastly, if neither grain refinement is achieved nor agglomeration of the oxide prevented, then we would conclude that the oxide agglomeration process is not prevented by the reduced gravity-driven convection currents. It is possible that convection currents

introduced by volume changes during solidification or by surface-tension effects (Marangoni Effect) may provide the collision-inducing velocity gradients which lead to agglomeration. These possibilities would have to be explored in an additional study.

The second set of low-g melting experiments, those in which potential nucleating agents are introduced into the beryllium powder compacts, will be aimed at obtaining further insight into nucleation during solidification and grain growth during cooling from the solidification temperature. These experiments should be especially helpful if the results of the first series of low-g experiments indicate that nucleation is the problem in obtaining fine-grain ingot beryllium.

It is anticipated that two series of melting experiments could be conducted, one series in the MSFC drop tower where the duration of the low-g portion of the drop is on the order of 3 or 4 seconds and a second series in a sounding rocket flight where the low-g duration is 5 to 7 minutes. The drop-tower experiments are less costly and more easily scheduled but may be rather limited in our experiments because of the necessarily high heating and cooling rates resulting from the requirement that melting and solidification be accomplished while at low g. The high heating and cooling rates and the resulting high thermal gradients might induce the undesired convection currents previously mentioned as arising from the variation of surface tension with temperature.

The slower heating and cooling rates possible in the longer duration sounding rocket flights would alleviate the threat of surface-tension-induced convection currents, would allow somewhat larger specimens to be used, and would ease inaccuracy problems associated with temperature measurement in a steep temperature gradient.

Because there are advantages of each of the two types of low-g experiments, we are suggesting that both types be conducted. All the experiments are the same in principle; the only difference will be the composition of the powder compacts, their geometry, and the heating and cooling apparatus and rates. In a typical experiment the sample will be preheated to $\sim$ 1000 C, then rapidly heated to above the melting temperature

(∿ 1450 C) as the sample enters the low-g portion of the experiments, and finally rapidly cooled so that solidification takes place while the specimen is still at low g. To prevent contamination, the specimens would have to be melted in BeO containers which should be rather thin walled to increase the heat-transfer rates. The BeO crucible capped with a BeO lid and containing a beryllium powder compact, which has previously been outgassed at 1000 C, will be hermetically sealed in a tantalum crucible at a vacuum of $\sim 1 \times 10^{-5}$ Torr. Both the drop tower and sounding rocket experiments will require continuous monitoring of the sample temperature in order to achieve the desired temperature and to obtain heating and cooling rate data which would be used in the analysis of the experiment.

In all cases the sample would be examined metallographically, and in the case of the beryllium powder compacts containing only the surface BeO, transmission electron microscopy (TEM) would be applied. The metallographic examination would be used primarily to determine whether the grain structure was finer than in samples comparably processed at 1 g. The TEM studies would be used to compare the degree of oxide agglomeration in the 1- and 0-g samples.

Drop Tower Experiments

It is contemplated that the experiments on both the beryllium powder compacts with and without the nucleating agent additions could be run in apparatus similar to that described by Reger and Hammel.[10] This unit allows for rapid heating and water quenching. It probably will be necessary to redesign and build a furnace system which would provide the higher temperatures needed in our experiment (1400-1500 C) and the rapid heating rate (160-250 C/sec) from the 1000 C preheat temperature. Protection from oxidation must also be provided to the tantalum sheathing by use of vacuum or inert atmosphere. An alternative to the use of an external coil-resistance element as a heat source would be to use the tantalum sheathing around the BeO crucible as the heating element. The close proximity of the tantalum sheath should allow efficient heat transfer into the BeO

crucible and melt. Provision must also be made for a thermocouple which enters the beryllium but which is protected by a tantalum sleeve coated on the otside with a thin layer of BeO. It is envisioned that the outside dimensions of the sample capsule would be approximately 1 cm in diameter by 1.3 cm long. A cooling rate from the melt temperature of $\geq$ 300 C/sec will be necessary to insure that the metal is solid before leaving the 0-g environment.

Sounding Rocket Experiments

It is expected that a sample geometry similar to that used in the current beryllium powder compact melting experiments could be used in the sounding rocket experiments. The furnace facility used in these experiments is capable of meeting the criteria that both melting and solidification are completely accomplished in the low-g portion of the rocket flight ($\sim$ 5 minutes). A power requirement of 840 watts (7 v - 120 amp) should allow the heating of the sample from 1000 C to 1450 C in $\sim$ 4 minutes. Radiation cooling should be sufficient to cool the sample from the maximum temperature to below the melting temperature (1283 C) in $\sim$ 1 minute, the remaining time at 0 g.

It, of course, would be necessary to modify the furnace to withstand the rigors of a rocket flight and to provide the proper power supply.

The specimen capsule design would be similar to that suggested for the drop tower experiments. The alternative option of heating the specimen by using the tantalum sheathing of the capsule as a furnace element should be viable in this case also.

REFERENCES

(1) Webster, D., Crooks, D. D., and Vidoz, A. E., "The Effect of Oxide Dispersions on the Recrystallization of Beryllium", Metall. Trans., 4 (1973) 2841.

(2) Markworth, A. J., Gelles, S. H., Duga, J. J., and Oldfield, W., "Immmiscible Materials and Alloys", paper presented at the Third Space Processing Symposium, Marshall Space Flight Center, Alabama (April 30 - May 1, 1974).

(3) Crossley, F. A., Metcalfe, A. G., and Graft, W. H., "Beryllium Research for Development in the Area of Casting", Wright Air Development Center, Technical Report 59-500 (July, 1959).

(4) Bibb, A. E., and Bishop, S. M., "Grain Refinement of Cast Beryllium", Report to the U.S. Atomic Energy Commission from Knolls Atomic Power Laboratory, Report No. KAPL-1917 (April 9, 1958).

(5) Crooks, D., and Sumsion, H., "Grain Refinement in Beryllium by Alloying", Lockheed Missiles and Space Division, Report LMSD-288233 (January, 1960).

(6) Chadwick, G. A., "Heterogeneous Nucleation of Metals From Their Melts", Metals and Materials (March, 1969) 77.

(7) Crosley, P. B., Douglas, A. W., and Mondolfo, L. F., "Interfacial Energies in Heterogeneous Nucleation", appearing in the Solidification of Metals, the Iron and Steel Institute (1968), Proceedings of the Conference in the Solidification of Metals held in Briton, England, December 4-7, 1967.

(8) Gelles, S., Nerses, V., and Siergiej, J., "Beryllium as a Structural Material", Journal of Metals (November, 1963) 843.

(9) Bunce, J.E.J., and Evans, R. E., "A Study of the Effect of Grain Size, Texture, and Annealing Treatment on the Properties of Wrought Beryllium Ingot", The Metallurgy of Beryllium, Chapman and Hall, Ltd., London (1963).

(10) Reger, J. L., and Hammel, R. L., "Experimental Development of Processes to Produce Homogenized Alloys of Immiscible Metals", Final Report Phase III to NASA, MSFC, Contract NAS8-27805, TRW Report No. 18677-6019-RU-00.